THE JOURNAL OF BIOLOGICAL CHEMISTRY VOL. 289, NO. 12, pp. 8337–8352, March 21, 2014

Cytochrome P450 2C Epoxygenases Mediate Photochemical Stress-induced Death of Photoreceptors*

Received for publication, August 5, 2013, and in revised form, February 4, 2014 Published, JBC Papers in Press, February 11, 2014, DOI 10.1074/jbc.M113.507152

Qing Chang[‡1], Evgeny Berdyshev[§], Dingcai Cao[‡], Joseph D. Bogaard[‡], Jerry J. White[¶], Siquan Chen[‖], Ravi Shah[‡], Wenbo Mu[‡], Rita Grantner[‖], Sam Bettis[‖], and Michael A. Grassi[‡2]

From the Departments of [‡]Ophthalmology and Visual Sciences and [¶]Research Resources Center and [§]Section of Pulmonary, Critical Care, Sleep and Allergy, University of Illinois, Chicago, Illinois 60612 and [‖]Institute for Genomics and Systems Biology, University of Chicago, Chicago, Illinois 60637

Background: New pharmacological entities are actively sought for treatment of inherited and age-related retinal degenerative diseases.
Results: Sulfaphenazole, a selective inhibitor of human cytochrome P450 (CYP) 2C9 enzyme, was identified as a novel cytoprotective agent against light-induced death of photoreceptors.
Conclusion: Cytochrome P450 CYP2C epoxygenases mediate photochemical stress-induced death of photoreceptors.
Significance: The CYP monooxygenase system is a risk factor for retinal photodamage.

Degenerative loss of photoreceptors occurs in inherited and age-related retinal degenerative diseases. A chemical screen facilitates development of new testing routes for neuroprotection and mechanistic investigation. Herein, we conducted a mouse-derived photoreceptor (661W cell)-based high throughput screen of the Food and Drug Administration-approved Prestwick drug library to identify putative cytoprotective compounds against light-induced, synthetic visual chromophore-precipitated cell death. Different classes of hit compounds were identified, some of which target known genes or pathways pathologically associated with retinitis pigmentosa. Sulfaphenazole (SFZ), a selective inhibitor of human cytochrome P450 (CYP) 2C9 isozyme, was identified as a novel and leading cytoprotective compound. Expression of CYP2C proteins was induced by light. Gene-targeted knockdown of CYP2C55, the homologous gene of CYP2C9, demonstrated viability rescue to light-induced cell death, whereas stable expression of functional CYP2C9-GFP fusion protein further exacerbated light-induced cell death. Mechanistically, SFZ inhibited light-induced necrosis and mitochondrial stress-initiated apoptosis. Light elicited calcium influx, which was mitigated by SFZ. Light provoked the release of arachidonic acid from membrane phospholipids and production of non-epoxyeicosatrienoic acid metabolites. Administration of SFZ further stimulated the production of non-epoxyeicosatrienoic acid metabolites, suggesting a metabolic shift of arachidonic acid under inhibition of the CYP2C pathway. Together, our findings indicate that CYP2C genes play a direct causative role in photochemical stress-induced death of photoreceptors and suggest that the CYP monooxygenase system is a risk factor for retinal photodamage, especially in individuals with Stargardt disease and age-related macular degeneration that deposit condensation products of retinoids.

Inherited retinal dystrophy and age-related macular degeneration (AMD)[3] are a devastating threat to public vision health worldwide. Retinitis pigmentosa (RP) is prevalent in inherited retinal dystrophy and is the leading cause of impaired vision and registered blindness in adults in many geographic locations, consuming substantial amounts of health resources and services in the United States (1–4). In contrast, AMD is more common in the elderly in developed countries and is prone to racial differences in prevalence (5–7). Currently, treatment options are limited for most conditions, and much effort has been devoted to delay progressive vision deterioration characterized by these diseases. For RP treatment, neurotrophic factors and cytokines (8–10), gene therapy/replacement (11, 12), antioxidants (13), and bone marrow-derived hematopoietic stem cells (14) have collectively been shown to have neuroprotective effects in genetic models of RP. However, direct translation of these findings into practical treatment of human RP patients has not been very successful. Some epidemiological studies show that dietary intake of vitamin A improves retinal function in RP patients (15). This practice, however, should be used with caution in patients with recessive RP and other related retinal diseases such as cone-rod dystrophy and Stargardt disease caused by *ABCA4* gene mutations because of the promotion effect of vitamin A on lipofuscin formation (16). For AMD treatment, antivascular endothelial growth factor therapy is approved by the Food and Drug Administration to treat neovascular AMD (17). To date, there is no approved treatment

* This work was supported, in whole or in part, by National Institutes of Health Grant EY001792, an NEI core grant. This work was also supported by funding from Hope for Vision, Foundation Fighting Blindness, Parent Petroleum, and Research to Prevent Blindness.
[1] To whom correspondence may be addressed: Dept. of Ophthalmology and Visual Sciences, University of Illinois, 1905 West Taylor St., Chicago, IL 60612. Tel.: 312-996-5865; E-mail: changq@uic.edu.
[2] To whom correspondence may be addressed: Dept. of Ophthalmology and Visual Sciences, University of Illinois, 1905 West Taylor St., Chicago, IL 60612. Tel.: 312-996-5865; E-mail: grassim@uic.edu.

[3] The abbreviations used are: AMD, age-related macular degeneration; SFZ, sulfaphenazole; CYP, cytochrome P450; EET, epoxyeicosatrienoic acid; AA, arachidonic acid; RP, retinitis pigmentosa; $\Delta\Psi m$, mitochondrial membrane potential; 5-HTR, 5-hydroxytryptamine receptor; PLA_2, phospholipase A_2; $AACOCF_3$, arachidonyl trifluoromethyl ketone; DHA, docosahexaenoic acid; RA, retinoic acid.

for atrophic AMD, which represents the majority of AMD cases. Antioxidants that remedy oxidative stress in AMD pathogenesis (18, 19) have benefited vision in patients with neovascular AMD but not in those with central geographic atrophy from a 10-year follow-up of the Age-Related Eye Disease Study (20). Thus, development of new routes with therapeutic potentials may provide new opportunities for treatment of RP and atrophic AMD.

A cell-based chemical screen has been applied to assist early phase drug discovery. This screen format is either based on the selection of a desirable phenotype or the readout of an introduced detection marker. By this approach, some prodrugs with potentials to treat neurodegeneration (21), cardiovascular diseases (22), and cancer (23, 24) have been developed. For therapeutic purposes, an advantage of the chemical screen is the bypass of *a priori* identification of disease-associated mutations or profound knowledge of pathogenesis. One example that fits this criterion is the cell viability/death screen by which neuroprotective compounds for treatment of stroke and ischemic brain injury as well as cytotoxic compounds for anticancer therapy have been discovered (25, 26). It would be even more valuable if the biosafety, bioavailability, and pharmacological actions of the compounds were available beforehand because a compendium of these characteristics would expedite the mechanistic investigation to identify the intervening targets or pathways as well as the process of clinical trials.

Light is an environmental risk factor for RP and AMD. Light can accelerate the progression and modify the course of RP (27). Animal models that replicate naturally occurring rhodopsin mutations of human autosomal dominant RP have a slowed recovery of rod function and greater degree of photoreceptor death by apoptosis in the inferior retina after light exposure (28–30). Other studies have shown that light-induced retinal damage in albino rats manifests histopathology and patterns of differential expression of disease-associated genes similar to those found in atrophic AMD (31–33).

We have shown previously that intense white light exposure causes death of mouse-derived photoreceptors (661W cells) by both necrosis and death receptor Fas-mediated apoptosis (34). Neutralizing Fas engagement with Fas ligand or inhibition of downstream effector caspases inhibits apoptosis but simultaneously aggravates cell death by necrosis. We propose that a cell-based chemical screen may help identify certain pleiotropic compounds capable to inhibit both necrosis and apoptosis. Hence, we conducted a positive selection screen of the Food and Drug Administration-approved Prestwick drug library in the phototoxicity model of 661W cells. We successfully identified a number of cytoprotective hits. One of the novel and leading hits, sulfaphenazole (4-amino-*N*-(1-phenyl-1*H*-pyrazol-5-yl)benzene-1-sulfonamide), a selective inhibitor of human cytochrome P450 (CYP) 2C9 enzyme, was chosen for mechanistic investigation. The results presented herein demonstrate a hitherto unacknowledged role of the CYP monooxygenase system in photochemical stress-induced death of photoreceptors.

EXPERIMENTAL PROCEDURES

Primary High-throughput Screening—Confluent 661W cells on 384-well plates (2.5×10^4 cells/well) were pretreated with the synthetic chromophore 9-*cis*-retinal (10 μM) overnight in 10% FBS, DMEM to increase the light sensitivity of these cells. The next day, the medium was exchanged with serum-free DMEM. The Prestwick drug library containing 1200 compounds was then added into the cells with a robotic arm at a final testing concentration of 10 μM for each compound. Each compound was tested in duplicate. After 2 h of incubation at 37 °C, the cells were exposed to fluorescent white light (11,000 lux) for 4 h. Controls included wells with medium only (blank), non-treated cells with light exposure on the same plate (negative control), and non-treated cells without light exposure in a separate plate (positive control). Cell viability was detected after light exposure using the redox-sensitive dye CellTiter Blue (Promega). Mean fluorescence, standard deviation, coefficient variation, and *Z* score were calculated (35).

Secondary Validation of Sulfaphenazole—Confluent 661W cells on 96-well plates were treated with serially diluted (0.625–100 μM) sulfaphenazole at 37 °C for 2 h. Minocycline and L-sulforaphane were co-tested separately at equivalent concentrations at the same time. Cells were then exposed to light for 4–6 h after which cell viability was detected using CellTiter-Glo (Promega), which measures cellular ATP according to the manufacturer's protocol. Luminescence was detected with a microplate reader at an integration time of 0.25 s/well.

Gene Silencing of CYP2C55 and CYP2C29—For siRNA-mediated gene silencing, 661W cells at 50% confluence on 96-well plates (for cell viability assay) or 6-well plates (for expression analysis of silencing efficiency) were transfected with different amounts (5–100 pmol) of Silencer Select predesigned siRNAs (Invitrogen) targeted to mouse CYP2C55 (sense, GGACAUUGACACUACUCCAtt; antisense, UGGAGUAGUGUCAAUGUCCtt), CYP2C29 (sense, CAAGGGAACUACAGUAAUAtt; antisense, UAUUACUGUAGUUCCCUUGgg), or scrambled negative control oligos using Lipofectamine RNAiMAX reagents (Invitrogen). At 48–72 h post-transfection, cells were processed for downstream experiments.

Generation of Stably Transfected CYP2C9-GFP Cell Lines in 661W Cells—661W cells at 50% confluence on 96-well plates were transfected with pCMV6-CYP2C9-GFP PrecisionShuttle mammalian expression vector (0.2 μg/well) using Turbofectin 8.0 (OriGene). Expression of CYP2C9-GFP fusion protein was under the control of the CMV promoter and Kozak sequence. Mock pCMV6-GFP-transfected 661W cells were controls. The parental pCMV6 vector expresses a neomycin resistance marker gene for positive selection of G418-resistant clones. 48 h post-transfection, cells from each transfected well were individually pooled and passaged in the presence of G418 at 450 μg/ml, an optimal concentration predetermined from a titration assay of G418 that kills wild-type, non-transfected cells within 2 weeks. The transfected cells were passaged and amplified under continuous G418 selection. Homogeneity of GFP-positive cells was examined by confocal microscopy using a FITC filter.

Enzymatic Assay of CYP2C9-GFP Fusion Protein—A cell-based luminogenic P450-Glo assay (Promega) was used to detect the enzymatic activity of CYP2C9-GFP fusion protein in pCMV6-CYP2C9-GFP stably transfected 661W cells. The assay is based on CYP2C9, which catalyzes a selective, cell-

permeable proluciferin substrate (luciferin-H) to generate luminogenic signal for detection. Endogenous cellular NADPH is provided as the electron donor for the reaction. Essentially, 661W cells were seeded on 96-well plates (5×10^3 cells/well) overnight in regular culture medium. The next day, the cells in some wells were pretreated with sulfaphenazole (10 μM) for 2 h at 37 °C. Substrate incubation, enzymatic assay, and luminescence detection all followed the manufacturer's protocol. Mock pCMV6-GFP stably transfected 661W cells and wild-type 661W cells were normal controls. Cell-free empty wells with luciferin-H were blank controls. Enzymatic activity was expressed as luminescence (relative light units)/h/5×10^3 cells after subtraction of background luminescence from blank controls.

Reactive Oxygen Species and Lipid Peroxidation Assays—Cellular hydroxyl radical ($^{\bullet}OH$) and superoxide anion ($O_2^{\bullet-}$) were detected using the oxidation-sensitive fluorescent dyes chloromethyl derivative of 2′,7′-dichlorodihydrofluorescein diacetate (488-nm excitation/535-nm emission) and dihydroethidium (495-nm excitation/595-nm emission) (Invitrogen), respectively. Light-exposed 661W cells on 96-well plates for different durations (15 min to 2 h) with/without sulfaphenazole pretreatment and control cells in the dark were washed with PBS. The fluorescent dyes (1 μM for each) predissolved in PBS were then added into the cells with incubation at 37 °C for 30 min. After incubation, the cells were washed again with PBS. Fluorescence was recorded with a microplate reader. In some experiments, the cells were also examined with a fluorescence microscope to evaluate consistency of the results.

For the lipid peroxidation assay, cellular malondialdehyde was detected using OxiSelect™ thiobarbituric acid reactive substances (Cell Biolabs, Inc.) according to the manufacturer's protocol. Serially diluted malondialdehyde was used to generate a standard curve.

Apoptotic and Necrotic Analysis—Fluorescence-activated cell sorting (FACS) by flow cytometry was conducted using Alexa Fluor 488-annexin V and propidium iodide (Invitrogen) as early apoptotic and necrotic markers, respectively. Fluorescent FLICA reagent (Invitrogen), which binds to the reactive cysteines of active caspase, was used to detect the activity of pan-caspases. 661W cells on 6-well plates were trypsinized, harvested by brief centrifugation ($500 \times g$ for 5 min), and finally resuspended in PBS. Alexa Fluor 488-annexin V and propidium iodide (1×100 dilution from stock for each) or 10 μl of 30× reconstituted FLICA reagent was added into cells with incubation at 37 °C for 15–30 min. After incubation, the cells were washed with PBS and centrifuged again. Fluorescence of cells in PBS suspension (400 μl/sample) was analyzed at 530 and 575 nm.

Mitochondrial Membrane Potential ($\Delta\Psi m$)—$\Delta\Psi$m was detected using the mitochondria-selective, lipophilic cationic dye 5,5′,6,6-tetrachloro-1,1′,3,3′-tetraethylbenzimidazolylcarbocyanine iodide (JC-1) (Cayman Chemical) according to the manufacturer's protocol. Fluorescence was recorded for the monomeric form of JC-1 (485-nm excitation/535-nm emission) that was higher in apoptotic cells with lower $\Delta\Psi$m.

Calcium Detection—Intracellular calcium was detected using the cell-permeable calcium-sensitive fluorescent dye Fluo-4 AM Direct (Invitrogen). Essentially, 661W cells were incubated with the dye (1 μM in calcium-free PBS) at 37 °C for 30 min. After incubation, Ca^{2+} fluorescence was detected by flow cytometry at 516 nm. Cells free of dye were controls. In some experiments, the Ca^{2+} fluorescence was re-evaluated in multiwell plate assays to increase the power of quantitative analysis. Blank wells and cells in wells free of dye were controls.

Arachidonic Acid and EET Analysis by Liquid Chromatography-Mass Spectrometry (LC/MS)—Lipids were extracted from conditioned medium (1 ml) and 661W cells (1.2×10^6 cells) using chloroform and methanol according to Bligh and Dyer (36). The organic phase was collected into glass tubes. The solvents were evaporated under a gentle stream of argon gas after which the dried residues were reconstituted in 50 μl of methanol/water (50:50, v/v). Commercial arachidonic acid and deuterated and non-deuterated EETs (Cayman Chemical) were used as internal standards.

For high performance LC-electrospray ionization-MS, an Agilent Technologies 1260 series HPLC system (Santa Clara, CA) consisting of a binary pump, an autosampler, and a thermostated column compartment was used with a Waters (Dublin, Ireland) BEH-C18 column (2.1×100 mm, 1.7 μm) for chromatographic separation of lipid samples and internal standards. Gradient elution began with an isocratic hold of the mobile phase, which consisted of 40% solvent A (0.1% formic acid) and 60% solvent B (100% acetonitrile) for 0.5 min. Solvent B was linearly increased to 75% at 2 min and then to 95% at 3.7 min and re-equilibrated until 7.5 min from the starting condition. The flow rate was 0.4 ml/min at 40 °C at an injection volume of 10 μl.

An AB Sciex QTRAP 5500 tandem quadruple mass spectrometer (San Jose, CA) was coupled to the HPLC system. Data were acquired in the negative ion mode with an electrospray ionization source using Analyst software version 1.5.1. Mass spectrometer conditions pertaining to the source/gas parameters (curtain gas (30.0), collision gas (medium), ion spray voltage (−4500 V), temperature (400 °C), and ion source gas 1 (25.0) and gas 2 (50.0)) as well as compound-specific parameters (declustering potential (150 V), collision energy (35 V), entrance potential (−5 V), and collision cell exit potential (−15 V)) were optimized by a continuous infusion of standard solutions via the instrument syringe pump system at a flow rate of 7 μl/min. Multiple reaction monitoring transitions were selected for each analyte of interest. A standard curve was generated at concentrations of 1, 2.5, 5, 10, 25, 50, 100, and 250 ng/ml internal standards for quantification of metabolites.

Western Blotting—Cell lysates were prepared from 661W cells using ProteoJET mammalian cell lysis reagent (Fermentas) containing 1:100 (v/v) protease inhibitor mixture (Roche Applied Science). The protein supernatants were cleared by centrifugation ($16{,}000 \times g$) at 4 °C for 15 min, heat-denatured, and separated by SDS-PAGE using 10% Mini-PROTEAN TGX gels (Bio-Rad). The proteins were transferred onto PVDF membrane, which was then blotted with rabbit-raised polyclonal anti-CYP2C9 (Sigma) primary antibodies at 1:2000 dilutions followed by incubation with HRP-conjugated secondary antibody (Santa Cruz Biotechnology) at 1:10,000 dilutions. Mouse monoclonal antibody against β-actin (Cell Signaling Technology) was used as a normalization control. Chemiluminescent signal was developed by ECL (GE Healthcare).

TABLE 1

Cytoprotective hit compounds against light stress

The compounds were extracted from the top 50 hits in the ranking list and arranged by pharmacological action and order of enrichment.

Pharmacological action	Compound name	Formula structure
Calcium/ion channel blockers	Ethosuximide	$C_7H_{11}NO_2$
	Dantrolene sodium salt	$C_{14}H_9N_4NaO_5$
	Tetracaine hydrochloride	$C_{15}H_{25}ClN_2O_2$
	Khellin	$C_{14}H_{12}O_5$
	Fendiline hydrochloride	$C_{23}H_{26}ClN$
	Dibucaine	$C_{20}H_{29}N_3O_2$
	Diazoxide	$C_8H_7ClN_2O_2S$
	Halofantrine hydrochloride	$C_{26}H_{31}Cl_3F_3NO$
	Indapamide	$C_{16}H_{16}ClN_3O_3S$
	Moricizine hydrochloride	$C_{22}H_{26}ClN_3O_4S$
	Dibucaine	$C_{20}H_{29}N_3O_2$
Dopamine receptor agonists	Apomorphine	$C_{34}H_{38}Cl_2N_2O_5$
	α-Santonin	$C_{15}H_{18}O_3$
	Metoclopramide	$C_{14}H_{23}Cl_2N_3O_2$
	Mefexamide hydrochloride	$C_{15}H_{25}ClN_2O_3$
	Pergolide mesylate	$C_{20}H_{30}N_2O_3S_2$
	Bupropion hydrochloride	$C_{13}H_{19}Cl_2NO$
Anti-inflammation drugs	Fenbufen	$C_{16}H_{14}O_3$
	Azapropazone	$C_{16}H_{20}N_4O_2$
	Triamcinolone	$C_{21}H_{27}FO_6$
	Piroxicam	$C_{15}H_{13}N_3O_4S$
	Minocycline hydrochloride	$C_{23}H_{28}ClN_3O_7$
	Dapsone	$C_{12}H_{12}N_2O_2S$
CYP inhibitors	Phensuximide	$C_{11}H_{11}NO_2$
	Isoniazid	$C_6H_7N_3O$
	Chloramphenicol	$C_{11}H_{12}Cl_2N_2O_5$
	Gemfibrozil	$C_{15}H_{22}O_3$
	Sulfaphenazole	$C_{15}H_{14}N_4O_2S$
Cytoskeleton/microtubule inhibitors	Griseofulvin	$C_{17}H_{17}ClO_6$
	Nocodazole	$C_{14}H_{11}N_3O_3S$
	Colchicine	$C_{22}H_{25}NO_6$
Protein synthesis inhibitors	Tetracycline hydrochloride	$C_{22}H_{25}ClN_2O_8$
	Gentamicin sulfate	$C_{60}H_{125}N_{15}O_{25}S$
	Chloramphenicol	$C_{11}H_{12}Cl_2N_2O_5$
Adrenergic receptor agonists/antagonists	Naftopidil dihydrochloride (α_1-adrenergic receptor antagonist)	$C_{24}H_{30}Cl_2N_2O_3$
	Guanfacine hydrochloride (α_2-adrenergic receptor agonist)	$C_9H_{10}Cl_3N_3O$
	Pindolol (partial β_3-adrenergic receptor agonist)	$C_{14}H_{20}N_2O_2$
Glucocorticoid receptor agonists	Triamcinolone	$C_{21}H_{27}FO_6$
	Dexamethasone acetate	$C_{24}H_{31}FO_6$
Serotonin receptor antagonist	Methiothepin maleate	$C_{24}H_{28}N_2O_4S_2$

Statistical Analysis—One-way analysis of variance (single factor) with α setting at 0.05 was performed to test the significance of means ± S.E. among multiple sample groups. Unpaired *t* test followed by adjustment with Bonferroni post hoc analysis was performed in two independent sample groups. A value of $p \leq 0.05$ was considered significant.

RESULTS

Pharmacological Classes of Cytoprotective Hits—We screened the Food and Drug Administration-approved Prestwick drug library containing 1200 bioactive compounds in a high throughput format to identify putative cytoprotective hits that may rescue light-induced death of the mouse-derived photoreceptors (661W cells) in culture. We ranked each of the compounds by calculating the *Z*-score (cutoff point >1) derived from cell viability assays that were performed after light exposure. We identified 61 compounds in total that met this criterion. The top 50 compounds from the ranking list were considered as hits and subjected to bio- and chemi-informatics analysis integrated with a literature search to query mechanism of action (Table 1 and Fig. 1). The analytic results revealed that ion channel blockers, cytochrome P450 (CYP) inhibitors, receptor agonists/antagonists, anti-inflammation drugs, protein synthesis inhibitors, and cytoskeletal and microtubule inhibitors represented the major classes of hits.

The intervening targets or pathways of some hits have previously been shown to be pathologically associated with RP, demonstrating the *in vivo* relevance of our model to disease pathogenesis. For example, ion (Ca^{2+}, Na^+, and K^+) channel blockers comprised the largest portion of hits (19%), reinforcing the importance of maintaining ion homeostasis for photoreceptor health. Loss-of-function mutations in the *PDE6* allele in *rd1* mice induce apoptosis in rods starting at early postnatal days (P10) due to Ca^{2+} overload via the cyclic nucleotide-gated channels (37, 38). A homozygous nonsense mutation in the voltage-gated K^+ channel subunit is genetically linked to human cone dystrophy (39). The mutually inclusive interaction between Ca^{2+} and K^+ is reiterated in isolated mouse retina in which a high K^+-induced depolarization of rods evokes Ca^{2+} influx (40).

Both dopamine receptor agonists and antagonists were identified as hits. The underlying mechanism by these two seemingly opposing actions of drugs may involve modulation of different aspects of dopamine signaling. Both stimulation and inhibition of dopamine signaling have been reported to protect photoreceptors from degenerative loss. For example, administration of dopamine D_2 receptor antagonists has been shown to preserve rods in retinal organ culture of *rd1* mice (41). Interestingly, it remains unclear how inhibition of dopamine signaling suppresses the underlying *PDE6* mutations that result in the overload of Ca^{2+} in rods. On the contrary, dopamine agonists have been shown to prevent light-induced retinal degeneration as a result of reciprocal inhibition of melatonin synthesis presumably through modulating the D_4 receptor in photoreceptors (42–46).

Two glucocorticoid receptor agonists (triamcinolone and dexamethasone acetate) were identified as hits. The underlying mechanism may involve activation of glucocorticoid receptor to repress the proapoptotic transcription factor AP-1 (47). Several anti-inflammatory compounds including the neuroprotective minocycline against light-induced retinal damage (48) represented another class of hits. Previous studies have shown that 661W cells release immunological molecules under light exposure to activate the resting retinal microglia (49). In assays using cytokine antibody array, we found that light-stressed 661W cells increased secretion of the chemotactic cytokine RANTES (regulated on activation normal T cell expressed and secreted) (data not shown), suggesting the possibility that *in vivo* damaged photoreceptors are able to activate and recruit resting retinal glial cells for neuroremodeling of retina in an active way similar to injured CNS neurons (50).

The serotonin receptor antagonist (methiothepin maleate) for 5-HT_1R and 5-HT_2R was the hit that targets to G-protein-coupled receptor. Pharmacological inhibition of 5-HT_2R attenuates light-induced retinal damage in *Abca4*$^{-/-}$*Rdh8*$^{-/-}$ mice that are defective in clearance of the visually toxic all-*trans* retinal released from photobleached rhodopsin (51). Several antihypertensive compounds such as naftopidil, guanfacine, and diazoxide were also identified as hits. The underlying mechanism may involve activation of the α_2-adrenergic receptor to

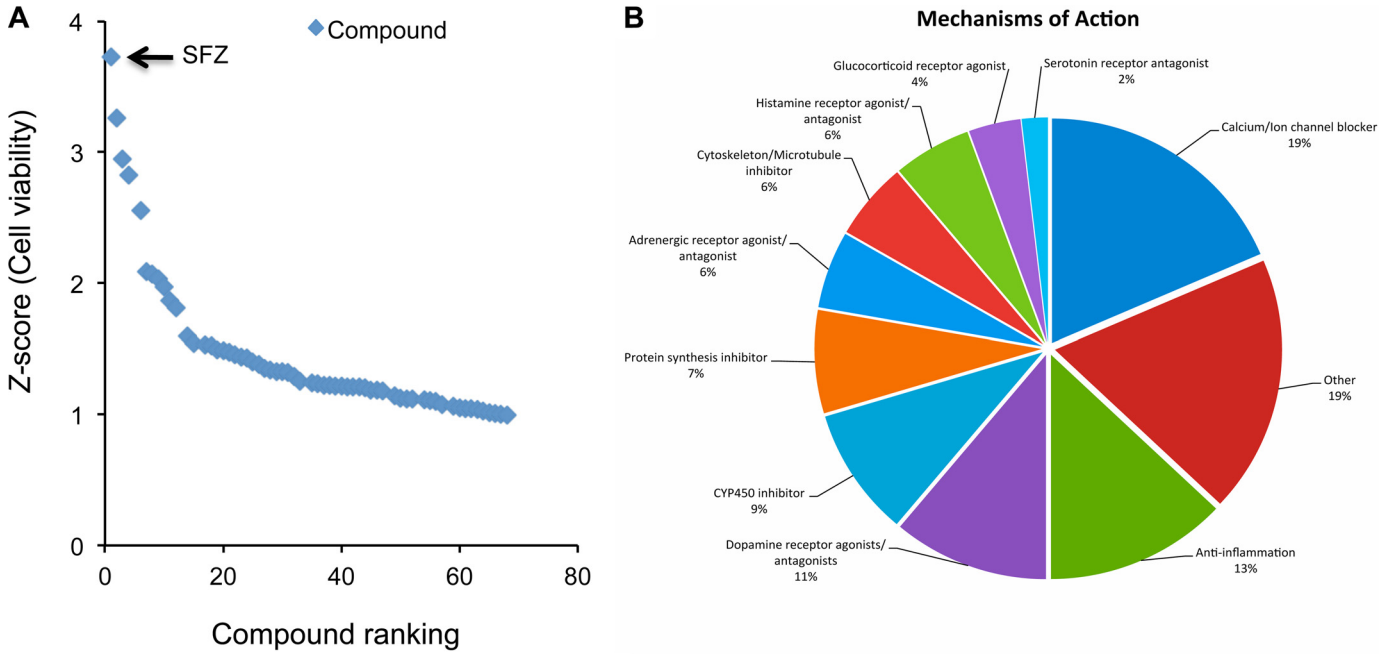

FIGURE 1. **Ranking and enrichment analysis of cytoprotective hit compounds.** Each compound was tested in duplicate in each run of the primary screen (total $n = 3$). Compounds were ranked by positive *Z*-scores (cutoff point >1) derived from fluorescence readings of cell viability assays after light exposure (*A*). The top 50 hits in the ranking list were grouped by pharmacological action derived from the DrugBank and PubChem database (*B*).

stimulate expression of the basic fibroblast growth factor in photoreceptors. Testing the neurotrophic response with these compounds in genetic models of RP may hold therapeutic value for neuroprotection. Compounds that inhibit CYP enzymes were another group of hits. Sulfaphenazole, a selective inhibitor of the human CYP2C9 enzyme, was identified as one of the leading hits. Other compounds that inhibit CYP enzymes in the hit list included phensuximide, an inhibitor of CYP2C19, and non-selective CYP inhibitors such as isoniazid, chloramphenicol, and gemfibrozil. Compounds that regulate organization and dynamics of cytoskeleton and microtubules were also identified as hits. In non-neuronal cells, cytoskeletal filaments can undergo both structural changes and abundant changes in response to activation of cell death programs (52). Because the small Rho GTPases are key regulators for many essential functions of the actin cytoskeleton (53), they may be involved in regulation of cell death pathways in photoreceptors.

Validation of Sulfaphenazole—We conducted a secondary screen to validate the cytoprotection of sulfaphenazole and compared its performance with two reported neuroprotective compounds: minocycline, a tetracycline derivative, and L-sulforaphane, an inducer of phase II detoxification enzymes (48, 54). Morphological examination of 661W cells after light exposure for 4 h showed that a fair number of cells pretreated with sulfaphenazole had elongated and spindle-like structures that are typical features of viable cells, whereas in non-treated cells or cells pretreated with minocycline or L-sulforaphane, most cells exhibited death phenotypes such as rounded, shrunken, and aggregated cell bodies with condensed nuclei (Fig. 2, *A–E*). To corroborate these morphological findings in a quantitative way, cellular ATP indicative of cell viability was measured. Sulfaphenazole demonstrated a dose-dependent increase of cellular ATP and better cytoprotective performance and durability than minocycline and L-sulforaphane (Fig. 2*F*). To test whether the cytoprotection is specific to sulfaphenazole, we tested ketoconazole, a broad spectrum CYP inhibitor, and cyclosporin A, an efficient inhibitor of CYP27A. Ketoconazole but not cyclosporin A also exhibited cytoprotection against light stress, suggesting a general causative role of the CYP enzymes in mediating cell death.

Gene Silencing of CYP2C55 Attenuates Light-induced Cell Death—We analyzed expression of mouse CYP2C isozymes in 661W cells. FASTA amino acid sequence alignment showed that mouse CYP2C55 and CYP2C29 are highly homologous to human CYP2C9 (74.4 and 75.7% identity and 91 and 93.7% similarity, respectively) (Fig. 3*A*). The Mouse Genome Informatics database (The Jackson Laboratory) lists mouse CYP2C55 as the homolog of human CYP2C9. Because of a lack of specific antibody, we used anti-human CYP2C9 antibody that cross-reacts with the mouse CYP2C homologs for detection of protein expression. A protein band slightly above the ~50-kDa molecular mass marker close to the predicted sizes of CYP2C55 (56 kDa) and CYP2C29 (55 kDa) was detected by Western blotting in 661W cells during normal growth in dark (Fig. 3*B*). Upon light exposure for 1–2 h without the cellular proteolysis that occurs at prolonged light exposure, expression of the CYP2C-like protein was induced (Fig. 3*B*, compare *lane 1* with *lanes 2–5*), suggesting a regulatory expression. Sulfaphenazole had no significant effect on expression under either light or dark exposure (Fig. 3*B* and data not shown). Because of uncertainty in isozyme specificity, we next took the siRNA-mediated gene silencing approach to tentatively target CYP2C55 or CYP2C29. Under the same transfection condition, expression of the CYP2C-like protein was significantly decreased when siRNA was targeted to CYP2C55 and mildly decreased when siRNA was targeted to CYP2C29 (Fig. 3*C*),

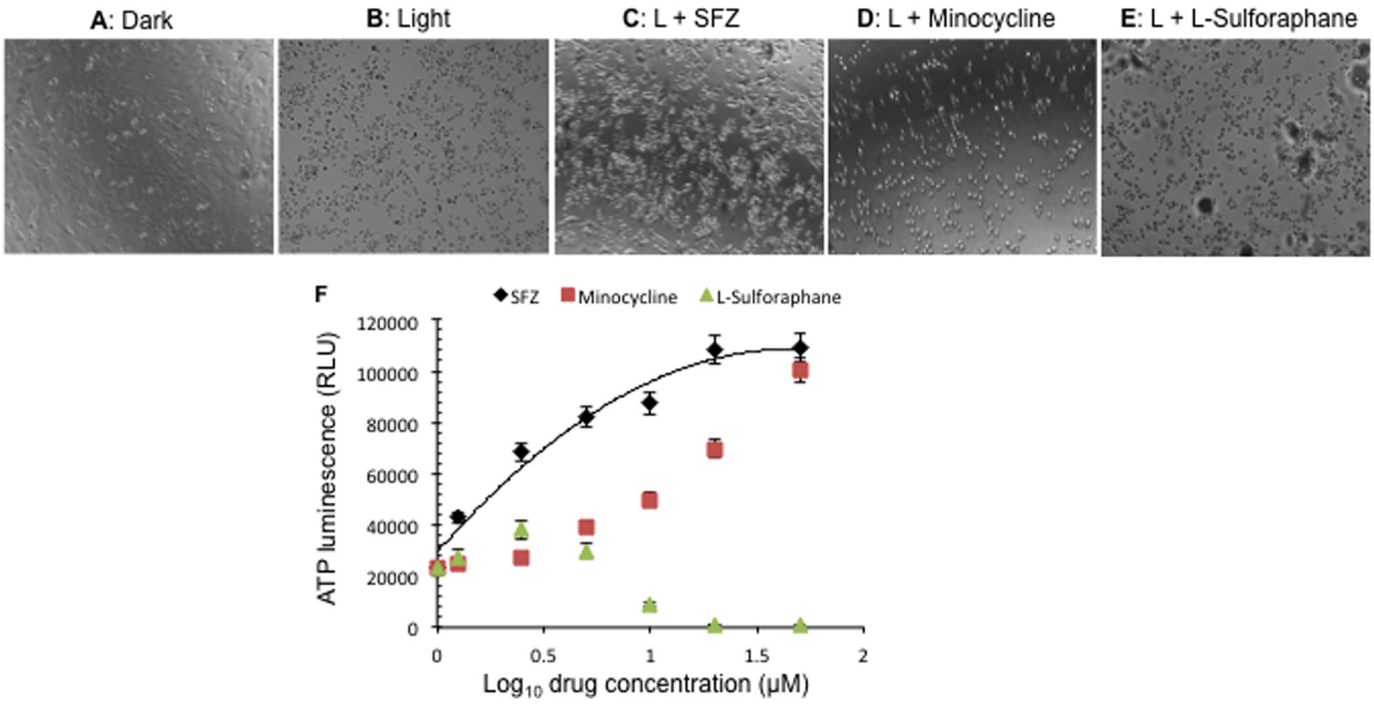

FIGURE 2. **Sulfaphenazole confers better cytoprotection than minocycline and L-sulforaphane.** 661W cells on 96-well plates were pretreated with serially diluted (0.625–100 μM) sulfaphenazole, minocycline, or L-sulforaphane ($n = 6$ concentrations/compound) for 2 h at 37 °C followed by light (*L*) exposure (11,000 lux) for 4 h. Cell morphology was examined intermittently during and after light exposure. Shown are the phase-contrast images at the end of light exposure at a working concentration of 10 μM for each compound together with non-treated positive (dark) and negative (light-exposed) control cells (*A–E*). Cellular ATP indicative of cell viability was measured after light exposure (*F*). *Error bars* represent means ± S.D. *RLU*, relative light units.

indicating that 661W cells express both CYP2C55 and CYP2C29 proteins. To assess the functional significance under gene silencing of CYP2C55 or CYP2C29, 661W cells were transfected with each targeted siRNA or mock transfected with the negative control oligo followed by light exposure and detection of cell viability (cellular ATP). The results revealed that knockdown of CYP2C55 or CYP2C29 did not affect cell viability during normal growth in the dark, suggesting that both are non-essential genes. In contrast, light-exposed cells with knockdown of CYP2C55 showed a significant improvement of cell viability (Fig. 3*D*), indicating a direct gene causative effect in cell death. The cytoprotection under knockdown of CYP2C29 was observed but did not reach statistical significance. This may be due to the insufficiency of gene silencing or actually a less causative effect in cell death.

Expression of Human CYP2C9 Enhances Cellular Sensitivity to Light—Given that gene silencing of CYP2C55 rescued light-induced death of 661W cells, we next examined whether expression of the homologous human CYP2C9 gene could enhance light sensitivity. The neuronal lineage of 661W cells limited achieving a high efficiency by transient transfection. Thus, we generated stably transfected CYP2C9 cell lines in 661W cells in which the CYP2C9 gene was expressed as a fusion protein with GFP at the C terminus (CYP2C9-GFP). Confocal microscopy examination of green fluorescence in live cells of stably transfected cells revealed that the majority of cells (~90% by fluorescence counting) were GFP-positive; albeit different fluorescence intensities were observed in some individual cells (Fig. 4*A*). This may be due to the different stages of the cell cycle that affect the expression level of GFP from the integrated expression vector. In some cells, expression of the CYP2C9-GFP fusion protein appeared surrounding the surface of the cell body. Although CYP enzymes are mainly localized in endoplasmic reticulum, plasma membrane-associated CYP2C9 has been reported and is catalytically active (55). In cell-based enzymatic assays, the CYP2C9-GFP fusion protein showed a concentration-dependent conversion of the selective substrate of CYP2C9 (luciferin-H) into a luminogenic product (Fig. 4*B*). Because it is unknown whether luciferin-H is a preferred substrate for mouse CYP2C isozymes, the endogenous enzymatic activity in wild-type cells was low by this assay approach. Pretreatment of CYP2C9-GFP stably transfected cells with sulfaphenazole dramatically inhibited the enzymatic activity to a low level virtually comparable with that of wild-type cells, suggesting that the GFP tag on the fusion protein does not nullify the selectivity of sulfaphenazole on the native CYP2C9 portion and reaffirming our results showing that the CYP2C9-GFP fusion protein was enzymatically active. In a functional evaluation, the CYP2C9-GFP stably transfected cells demonstrated a remarkably increased sensitivity to light-induced cell death as compared with wild-type cells (Fig. 4*C*) or mock GFP stably transfected cells (data not shown). Pretreatment of CYP2C9-GFP stably transfected cells with sulfaphenazole improved cell viability, but viability did not surpass that of light-exposed wild-type cells. Together, these collective functional data indicate that the human CYP2C9 gene plays a specific and synergistic role in mediating light-induced cell death.

Sulfaphenazole Inhibits Light-induced Necrosis and Apoptosis—We showed previously that light-induced death of 661W cells involves both necrosis and apoptosis (34). To deter-

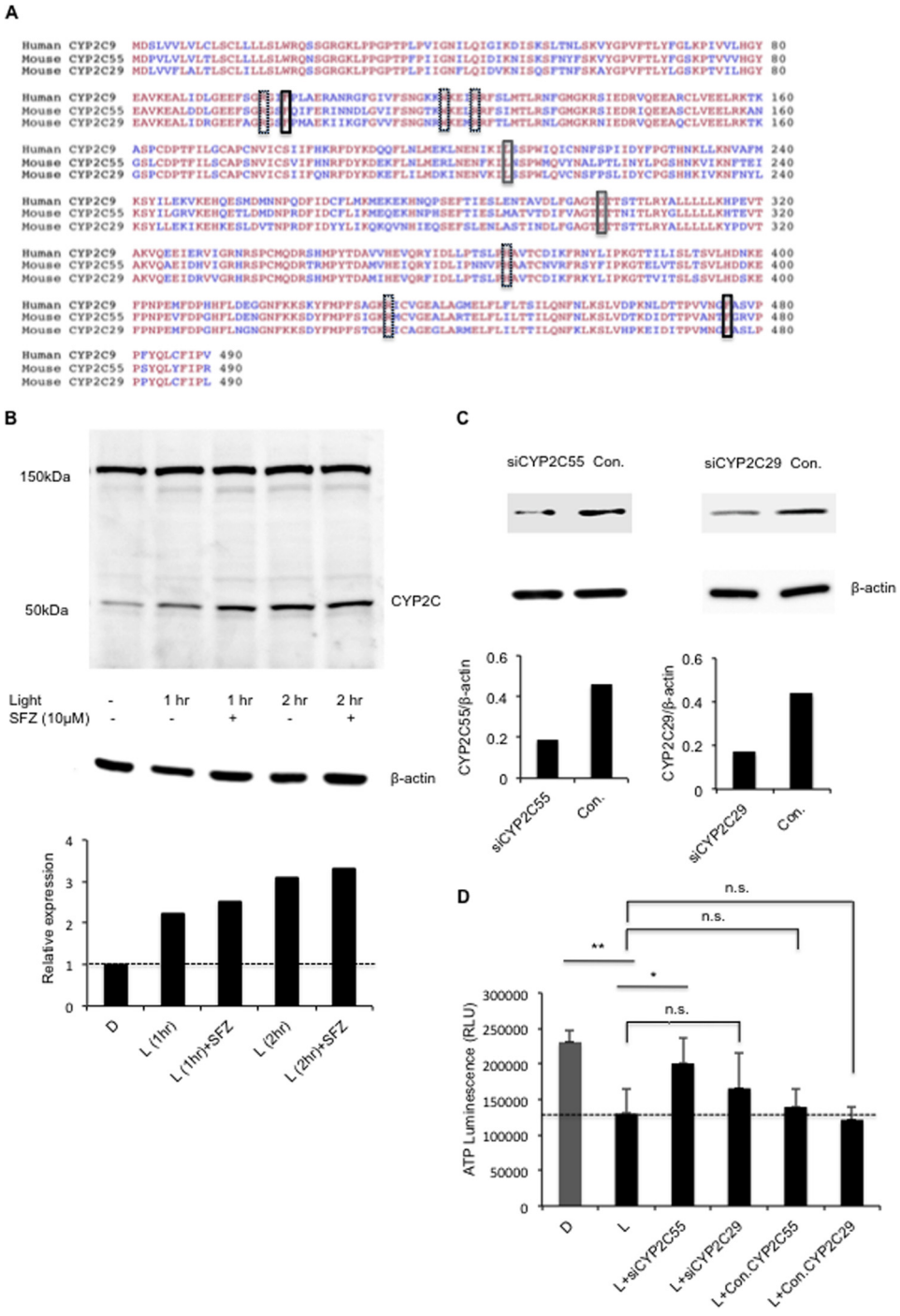

FIGURE 3. **Expression of CYP2C is inducible by light and targeted knockdown of CYP2C55 rescues light-induced cell death.** Deduced amino acids of encoded human CYP2C9 and mouse CYP2C55 and CYP2C29 enzymes were aligned using Clustal Omega. *Rectangular boxes* represent key conserved residues for catalytic activity (*gray*), ligand binding (*black*), and heme stabilization (*dashed*) (see Ref. 90) (*A*). 661W cells on 6-well plates with/without sulfaphenazole pretreatment for 2 h at 37 °C were exposed to light (*L*) or remained in the dark (*D*). Expression of CYP2C proteins was detected from prepared cell lysates by Western blotting using anti-human CYP2C9 polyclonal antibody that cross-reacts with mouse CYP2C isozymes. The housekeeping gene β-actin was used as a loading control. Relative expression is presented by normalization with the densitometric ratio of CYP2C/β-actin in dark control cells (*B*). 661W cells at 50% confluence were transfected with Silencer Select predesigned siRNAs targeted to mouse CYP2C55 or CYP2C29 or mock-transfected with the scrambled control (*Con.*) oligos ($n = 4$/sample group). Cell lysates were prepared at 48 h after transfection to assess silencing efficiency by Western blotting. The densitometric ratio of CYP2C55 or CYP2C29/β-actin is presented (*C*). Cellular ATP indicative of cell viability was measured after light exposure ($n = 4$/sample group) (*D*). **, $p < 0.01$; *, $p < 0.05$; *n.s.*, not significant. *RLU*, relative light units. In *B*, *bars* represent the relative ratio of densitometry (CYP2C/β-actin) from one representative experiment. In *C*, *bars* represent the absolute ratio of densitometry (siCYP2C55 or siCYP2C29/β-actin).

mine whether sulfaphenazole inhibits either one or both of the two cell death programs, we conducted FACS analysis by flow cytometry in light-exposed 661W cells using fluorescence-labeled annexin V and propidium iodide. The results revealed that light exposure resulted in about a 1.27-fold increase in the number of apoptotic cells (+annexin V) and a 2.85-fold increase in the number of necrotic cells (+annexin V/+propidium iodide) as compared with the dark control cells (Fig. 5, *A*

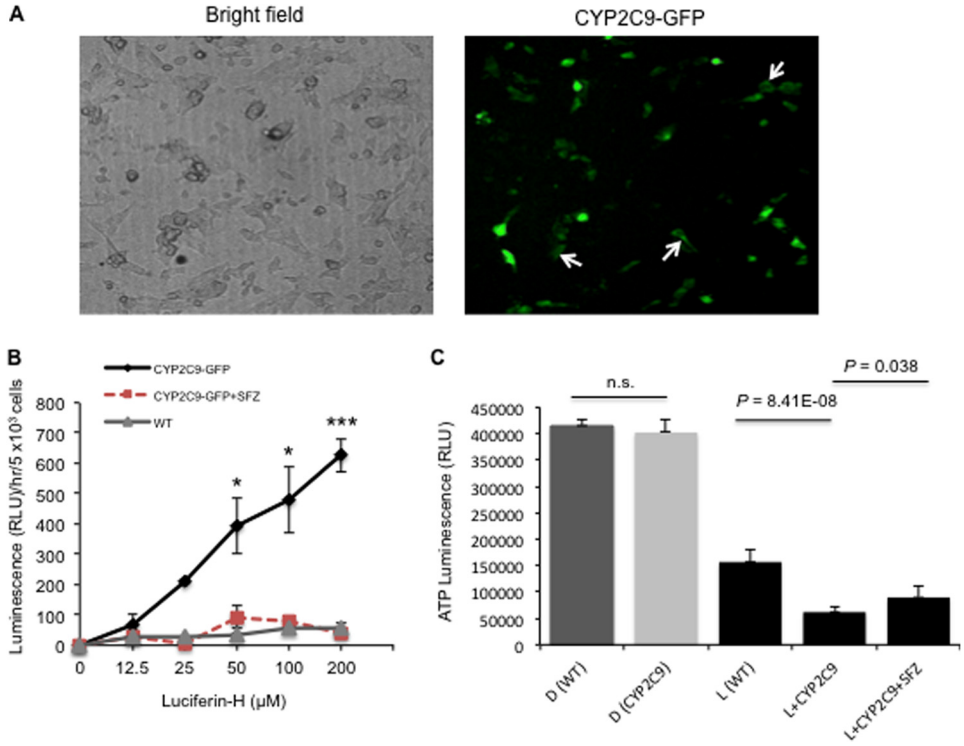

FIGURE 4. **Stable expression of functional human CYP2C9-GFP fusion protein enhances cellular sensitivity to light.** pCMV6-CYP2C9-GFP stably transfected 661W cells were examined by confocal microscopy showing the bright field and its switch to FITC mode to assess homogeneity of GFP-positive cells. The *arrow* indicates expression of CYP2C9-GFP on the surface of the cell body (*A*). The enzymatic activity of CYP2C9-GFP fusion protein with/without sulfaphenazole (10 μM) pretreatment was examined by a cell-based luminogenic assay that generates luminogenic signal from CYP2C9-catalyzed oxidation of the selective substrate luciferin-H. Wild-type (WT) 661W cells were controls. $n = 3$/luciferin-H concentration. ***, $p < 0.001$; *, $p < 0.05$ *versus* CYP2C9-GFP + SFZ (*B*). pCMV6-CYP2C9-GFP stably transfected 661W cells with/without pretreatment with sulfaphenazole (10 μM) ($n = 12$/treatment or non-treatment group) and wild-type cells ($n = 24$) were exposed to light for 4 h. Cellular ATP indicative of cell viability was measured after light (*L*) exposure (*C*). *n.s.*, not significant. *Error bars* represent means ± S.D. *RLU*, relative light units; *D*, dark.

and *B*, compare the *R6* and *R4* regions). In cells pretreated with sulfaphenazole, the numbers of light-induced apoptotic and necrotic cells were decreased by 33 and 44%, respectively (Fig. 5*C*, compare *R6* and *R4* regions with the same regions in *B*). Quantitation of apoptotic and necrotic cells is presented in Fig. 5*D*. To further corroborate this finding, the activity of pan-caspases (most initiator and executioner caspases) was detected by affinity labeling using the FLICA reagent. Increased FLICA fluorescence by a right shift in the histogram was found in light-exposed cells, indicating activation of pan-caspases. In contrast, a largely diminished intensity of FLICA fluorescence was observed in cells pretreated with sulfaphenazole (Fig. 5, *E–G* and *H* for quantitation). To investigate whether the inhibition of pan-caspases by sulfaphenazole arises from prevention of mitochondrial stress, the $\Delta\Psi$m was detected. A lower $\Delta\Psi$m was observed in light-exposed cells, whereas in cells pretreated with sulfaphenazole, the $\Delta\Psi$m was significantly restored (Fig. 5*I*). Together, these coherent results from a series of independent experiments demonstrate that sulfaphenazole has both antiapoptotic and antinecrotic properties.

Sulfaphenazole-targeted CYP(s) Does Not Cause Oxidative Stress—Certain CYP-catalyzed oxidation reactions generate reactive oxygen species due to poor coupling of the catalytic cycle (56, 57). In addition, under intense light exposure, photoreceptors may experience photo-oxidative stress. To test whether sulfaphenazole has an antioxidative function, $O_2^{\cdot-}$ and $^{\cdot}OH$ were detected in a time course experiment of light (15 min to 2 h) prior to massive death at a later time. Light exposure did not significantly change the $O_2^{\cdot-}$ level in cells when compared with that in dark control cells. Interestingly, the $O_2^{\cdot-}$ level in light-exposed cells that had been pretreated with sulfaphenazole was substantially reduced (Fig. 6*A*). In contrast, the $^{\cdot}OH$ level was found to be even higher in dark control cells than in light-exposed cells. Pretreatment of cells with sulfaphenazole had no significant effect on the $^{\cdot}OH$ level under light exposure (Fig. 6*B*). This higher basal level of $^{\cdot}OH$ may result from the reactive nature of the preadded synthetic chromophore 9-*cis*-retinal. When the cells were shifted to light exposure, $^{\cdot}OH$ might have been buffered by up-regulation of antioxidative and redox genes (58, 59). This interpretation was justified by the correlated increase of the lipid peroxidation product, malondialdehyde, in cells under dark exposure and its decreased production under light exposure (Fig. 6*C*). To further evaluate whether photo-oxidative stress contributes to cell death, the cells were pretreated with antioxidants *N*-acetylcysteine, vitamin C, vitamin E, and dimethylthiourea either singly or in combination prior to light exposure. No appreciable cytoprotection was observed (data not shown), indicating that photo-oxidative stress is not a primary factor for cell death. Although sulfaphenazole reduced the cellular $O_2^{\cdot-}$ level in light-exposed cells, this cannot explain its cytoprotective mechanism because of the higher burden of oxidative stress in dark control cells. Nonetheless, a concomitant inhibition of $O_2^{\cdot-}$ by sulfaphenazole may bestow a beneficial role for cell recovery from light stress.

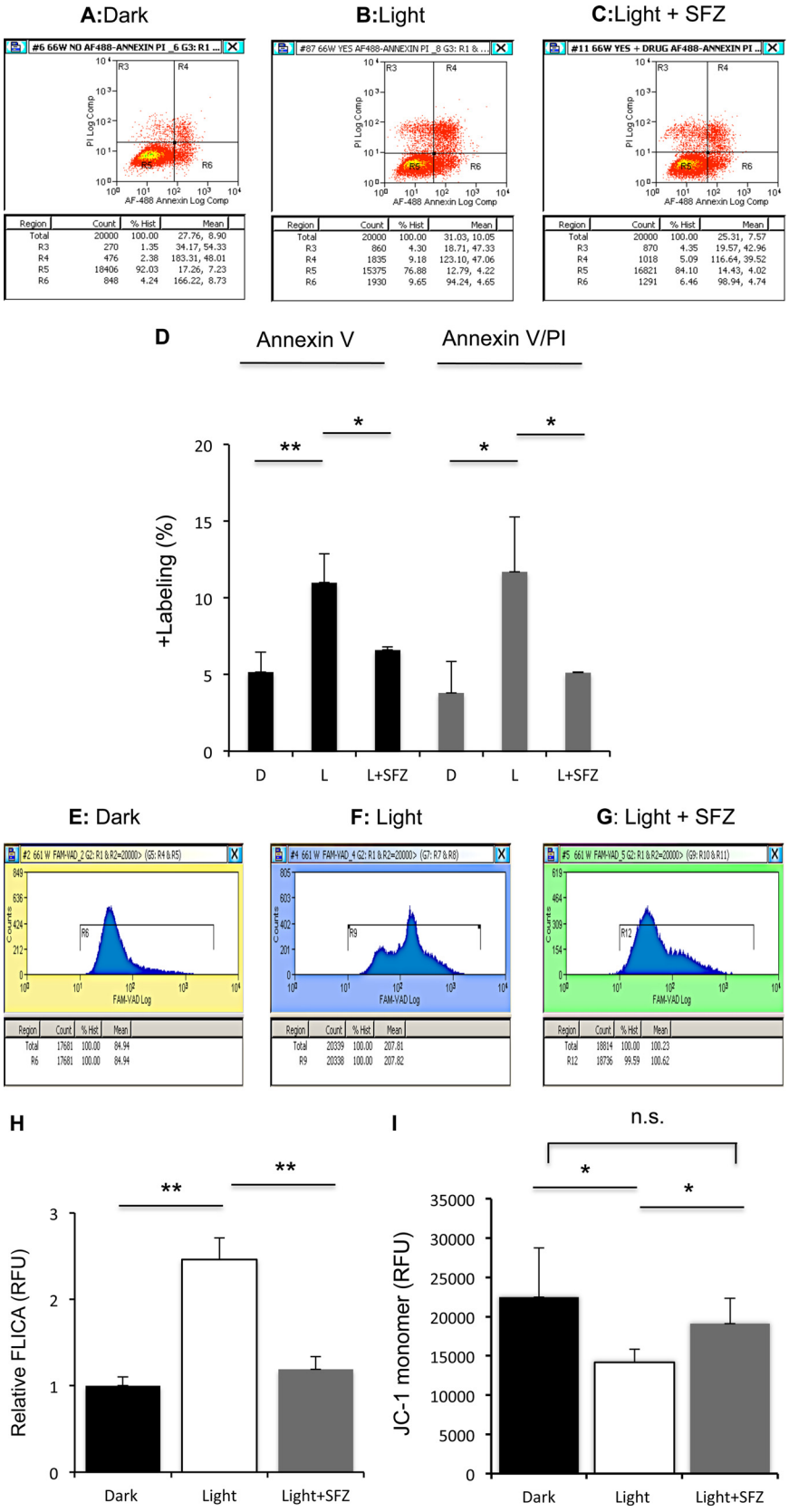

FIGURE 5. **Sulfaphenazole inhibits light-induced necrosis and apoptosis.** 661W cells were pretreated with/without sulfaphenazole for 1 h at 37 °C followed by light exposure for 2–3 h. Within this time window, we usually observed a peak of apoptosis. Apoptotic and necrotic cells were detected by flow cytometry using Alexa Fluor 488-conjugated annexin V and propidium iodide, respectively. Histograms are shown (*A–C*; $n = 3$/sample group). Quantitation is shown in *D*. The activity of pan-caspases was independently detected using FLICA reagent ($n = 5$/sample group) (*E–G*). Quantitation is shown in *H*. $\Delta\Psi$m was detected using the mitochondrion-selective fluorescent dye JC-1 ($n = 10$/sample group) (*I*). **, $p < 0.01$; *, $p < 0.05$; *n.s.*, not significant. *Error bars* represent means ± S.D. *RFU*, relative fluorescence units; *L*, light; *D*, dark.

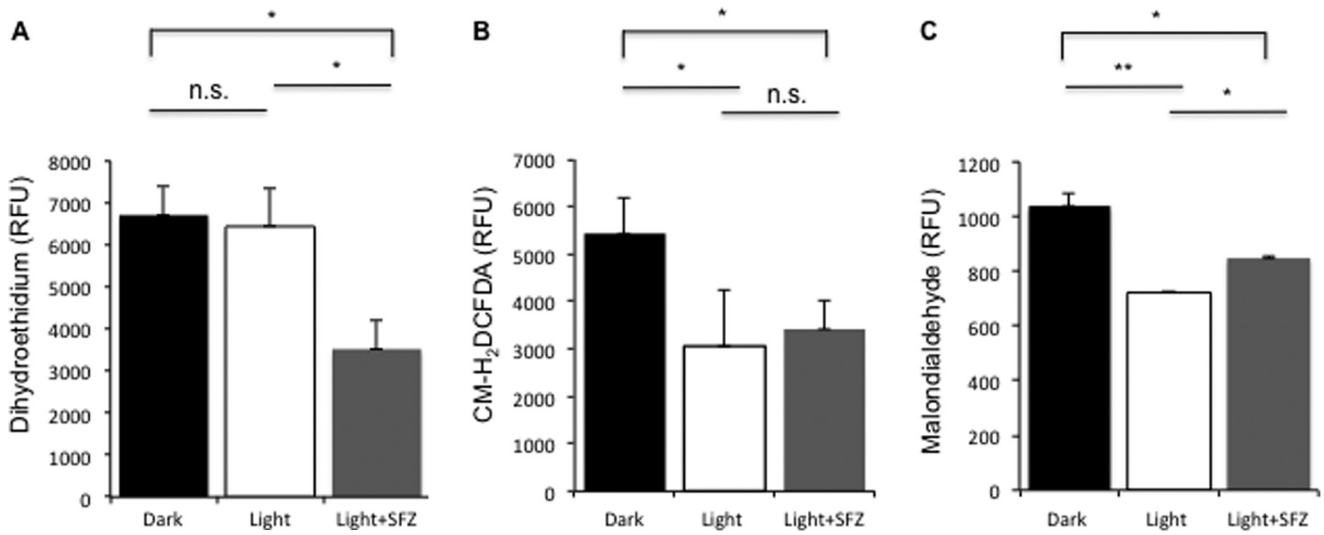

FIGURE 6. **Sulfaphenazole reduces O_2^- production.** Cellular O_2^- ($n = 6$/dark control group, $n = 9$/light- or SFZ-treated group) (*A*) and $^{\cdot}OH$ ($n = 6$/dark control group, $n = 9$/light- or SFZ-treated group) (*B*) were detected using the oxidation-sensitive dyes dihydroethidium and chloromethyl derivative of 2′,7′-dichlorodihydrofluorescein diacetate (*CM-H_2DCFDA*), respectively. Data are shown at 2 h of light exposure. The lipid peroxidation product malondialdehyde was detected by thiobarbituric acid reactive substances assay in separate samples ($n = 4$/sample group) (*C*). **, $p < 0.01$; *, $p < 0.05$; *n.s.*, not significant. *Error bars* represent means ± S.D. *RFU*, relative fluorescence units.

Sulfaphenazole Mitigates Light-induced Calcium Influx—Light-illuminated retina stimulates phospholipase A_2 (PLA_2)-mediated release of arachidonic acid (AA) from membrane phospholipids (60). The responsible retinal cells, however, are unknown. Some secretory forms of PLA_2 are expressed in photoreceptors, and their expression is induced by light (61). These lines of evidence together with the endogenous expression of CYP2C55 and CYP2C29 in 661W cells (Fig. 3) suggest the possibility that light may stimulate production of CYP2C isozyme-generated eicosanoid metabolites of AA. Regioselective epoxyeicosatrienoic acids (EETs) promote capacitative calcium entry (62). Thus, we hypothesized that sulfaphenazole may affect calcium flux in 661W cells under light stress. Excessive calcium influx induces both necrosis and apoptosis (63, 64). As a proof of concept, we first evaluated whether there is a dynamic change of intracellular calcium during light exposure. Indeed, time course experiments revealed an increase of intracellular calcium at 2 h of light exposure (Fig. 7, *A* and *B*, compare the mean and *R* values, and data not shown). Cells pretreated with sulfaphenazole showed a substantial reduction of light-induced calcium influx (Fig. 7*C*, compare the mean and *R* values with those in *B*). If inhibition of CYP2C-generated eicosanoids by sulfaphenazole is involved in light-induced calcium influx, then prevention of PLA_2-mediated release of AA from membrane phospholipids may exert a similar effect. To test this possibility, 661W cells were pretreated with the cytosolic and Ca^{2+}-independent PLA_2 inhibitor $AACOCF_3$ (an analog of AA). $AACOCF_3$-treated cells showed a reduction of intracellular calcium (Fig. 7*D*, compare the mean and *R* values with those in *B*); however, it did not reach statistical significance. To test the participation of cyclooxygenases and lipoxygenases in light-induced calcium influx, the cells were pretreated with their respective inhibitors: diclofenac sodium and caffeic acid. Neither of the two inhibitors showed an appreciable effect (data not shown). Together, these pharmacological results suggest that the antinecrotic and antiapoptotic properties of sulfaphenazole are mediated at least partially through prevention of calcium-mediated cytotoxicity.

Light Provokes Release of AA and Its Non-EET Metabolites—Next, we investigated whether light affects PLA_2-mediated release of AA and its metabolites in 661W cells. Using LC/MS, we quantitatively measured and compared the cellular free AA and four *cis*-regioisomers (14,15-; 11,12-; 8,9-; and 5,6-) of EETs under dark and light exposure. The results revealed that light-exposed cells significantly increased release of AA as compared with dark control cells (area/volume, 2.18E+04; concentration, 1.04 μg/ml in dark *versus* area/volume, 7.90E+04; concentration, 3.76 μg/ml in light) (Fig. 8, *A* and *B*). The magnitude of AA abundance was further increased after light-exposed cells were additionally incubated in the dark overnight (area/volume, 2.63E+05; concentration, 12.52 μg/ml), suggesting an extended release (Fig. 8*C*). Under light exposure, we found that two metabolites with matching mass/transition ion pairs to 8,9- and 14,15-EETs at *m*/*z* 319/167 and *m*/*z* 319/219, respectively, were significantly increased both in the conditioned medium and in cells after normalization with total lipid phosphates (Table 2 and Fig. 8, *D–F*). In particular, the metabolite with *m*/*z* 319/167 increased 6.2-fold in the conditioned medium and 9.5-fold in cells, and the metabolite with *m*/*z* 319/219 increased 3.5-fold in the conditioned medium and 2-fold in cells. Administration of sulfaphenazole further increased the production of the two metabolites. Specifically, the metabolite with *m*/*z* 319/167 increased 41% in conditioned medium and 55% in cells. Under the same condition, the metabolite with *m*/*z* 319/219 increased 42% in the conditioned medium and increased as high as 3-fold in cells. The retention time of *m*/*z* 319/167 and *m*/*z* 319/219, however, was slightly shorter (<0.1 min) than that from the deuterated internal standards. To further elucidate whether the two metabolites are authentic EETs or other non-EET metabolites, we detected all transition ions common or unique to known *cis*-regioisomers of EETs (Table 3). With the profile of these transition ions available, we

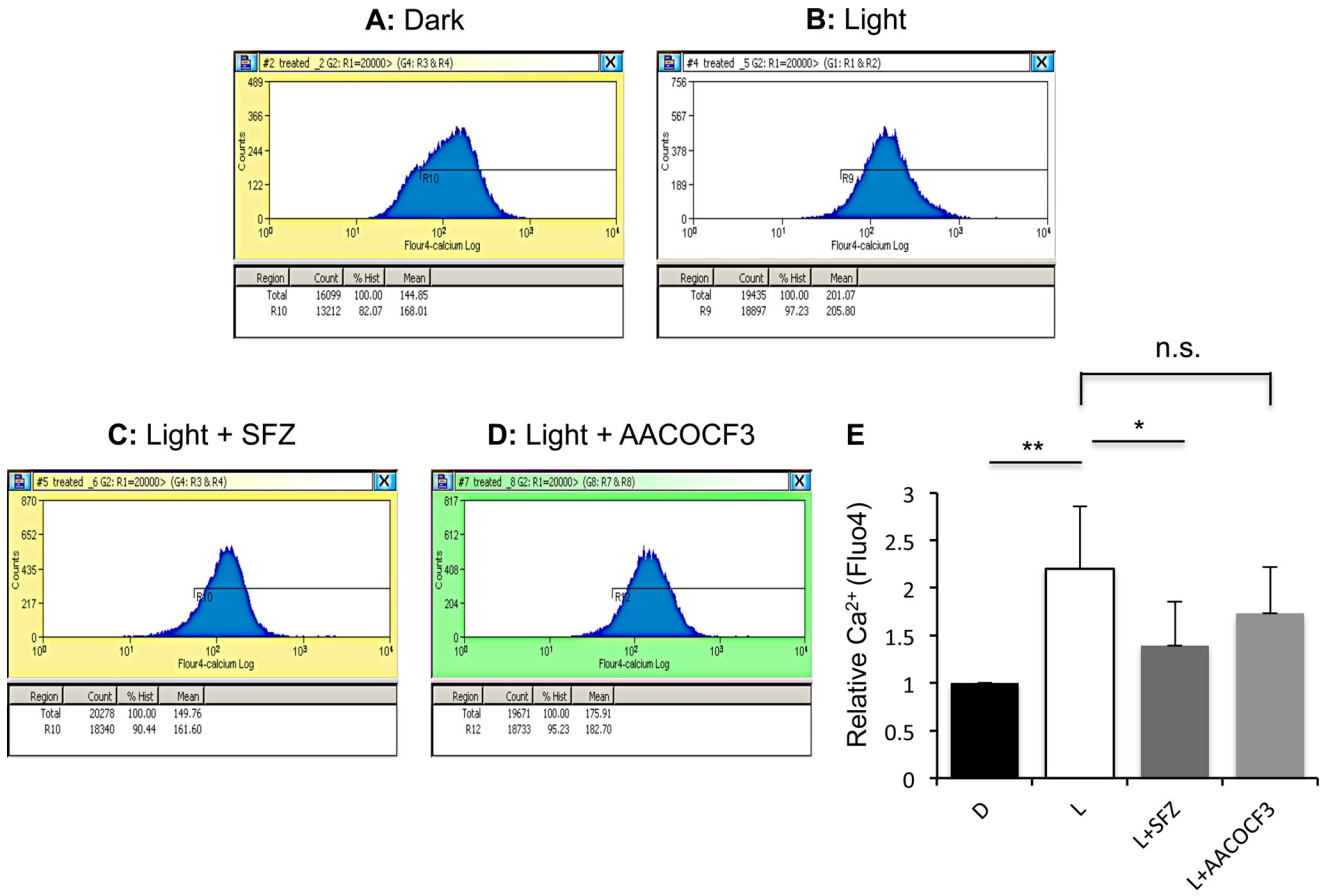

FIGURE 7. **Sulfaphenazole inhibits light-induced calcium influx.** 661W cells were pretreated with sulfaphenazole or PLA_2 inhibitor $AACOCF_3$ ($n = 4$/sample group) for 1 h at 37 °C followed by light exposure for 2 h. Intracellular calcium was detected by flow cytometry using the calcium-sensitive fluorescent dye Fluo-4 AM Direct (1 μM) for control cells (*A*), light-exposed cells (*B*), light-exposed cells + SFZ (*C*), and light-exposed cells + $AACOCF_3$ (*D*). **, $p < 0.01$; *, $p < 0.05$; *n.s.*, not significant. *Error bars* represent means ± S.D. *L*, light; *D*, dark.

repeated the experiment but were unable to identify other common or unique transition ions of EETs either in the condition medium or in cells under light exposure, suggesting that the two metabolites are not authentic EETs but have the same molecular mass as EETs and can create certain identical transition ions. Collectively, results from our LC/MS analysis indicate that light-stressed photoreceptors trigger an increased release of AA and production of its non-EET metabolites. Administration of sulfaphenazole further stimulates the production of non-EET metabolites, suggesting a metabolic shift of AA under inhibition of the CYP2C pathway.

DISCUSSION

Sulfaphenazole was initially reported as a selective inhibitor of human CYP2C9 and was shown to inhibit other human CYP2C isozymes much less potently (65). In this study, we identified sulfaphenazole as a novel cytoprotective compound in a chemical screen against light-induced death of the mouse-derived photoreceptor cell line (661W cells). 661W cells exhibit biochemical properties of cones and express cone-specific pigments, transducin, and arrestin. Morphologically, these cells do not have outer segment structures in culture. Given the uniformity of cell growth and maintenance of cone-specific markers during passages, this cell line is well suited for a cell-based high throughput screen. Following the primary screen of the Food and Drug Administration-approved drug library, we performed a series of experiments to validate the cytoprotection of sulfaphenazole and to characterize its mechanistic action. Our results indicated that sulfaphenazole is a pleiotropic compound. It inhibits light-induced necrosis and mitochondrial stress-initiated apoptosis in 661W cells. This antinecrotic and antiapoptotic property may partially result from prevention of light-induced calcium influx. The results of our study implicate the monooxygenase CYP system as a risk factor for retinal photodamage.

The exact target of sulfaphenazole on mouse CYP2C isozymes remains unclear. The mouse genome contains more CYP2C genes than does the human genome (15 CYP2C genes in mouse *versus* four CYP2C genes in human). Accordingly, this naturally introduces a level of complexity whether sulfaphenazole targets a single or more than one mouse CYP2C isozyme. The high degree of sequence homology and similarity of mouse CYP2C55 and human CYP2C9 implies that it is a candidate target. This presumption is supported from a functional standpoint by our results showing that gene-targeted knockdown of CYP2C55 conferred cytoprotection to light-induced cell death, whereas stable expression of functional human CYP2C9-GFP fusion protein further sensitized cells to toxic light (Figs. 3 and 4). These two reciprocal findings establish a direct gene causative role

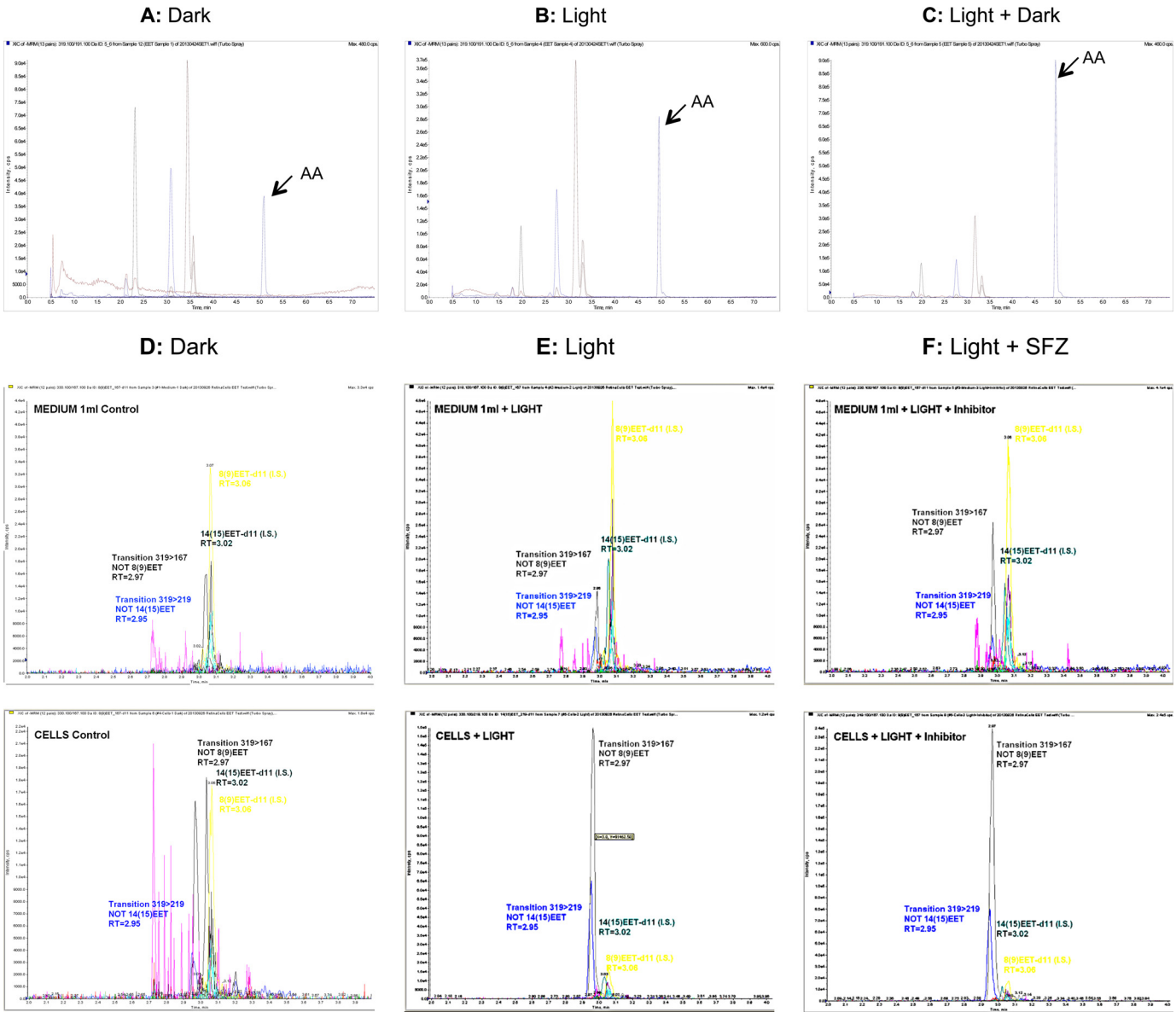

FIGURE 8. **Light increases release of AA and non-EET metabolites.** Lipids from conditioned medium or cells were quantitatively analyzed by LC/MS (see "Experimental Procedures"). Chromatographs are shown for free AA in dark control cells (*A*), 4-h light-exposed cells (*B*), and light-exposed cells with additional dark incubation overnight (*C*). In our original hypothesis, we analyzed four *cis*-regioisomers of EETs from metabolism of AA. Chromatographs are shown for two metabolites with the same molecular mass and transition ions (*m/z* 319/167; *gray* peak) and (*m/z* 319/219; *blue* peak) as 8,9- and 14,15-EETs, respectively, in the conditioned medium and cells in dark (*D*), after light exposure (*E*), or with SFZ pretreatment (10 μM) (*F*). Note that the retention time of the two metabolites was slightly shorter than (<0.1 min) that generated by the deuterated 8,9-EET (*yellow* peak) and 14,15-EET (*green* peak) internal standards.

TABLE 2

Light increases AA metabolites with same mass to EETs

Lipids were extracted from conditioned medium and cells under dark or light exposure with/without pretreatment with sulfaphenazole. LC/MS quantitative analysis was performed using deuterated EETs as internal standards. Results were normalized with total lipid phosphates (P).

	Medium			Cells		
	Dark	Light	Light + SFZ	Dark	Light	Light + SFZ
	fmol/nmol lipid P			*fmol/nmol lipid P*		
Metabolite with *m/z* 319/167	0.05	0.31	0.44	0.8	7.6	11.83
Metabolite with *m/z* 319/219	0.02	0.07	0.1	0.03	0.06	0.18

in mediating cell death and suggest functional similarity of the two homologous CYP2C genes between mouse and human.

Our findings do not suggest photo-oxidative stress as a primary mechanistic factor for cell death. There are three lines of evidence that support this conclusion. First, compounds with antioxidative activity such as minocycline, niacin, and vitamin K_2 were not identified as top cytoprotective hits during the primary screen. Second, compared with dark control cells, the light-exposed cells did not show elevation of hydroxyl radical, superoxide anion, and the lipid peroxidation product, malon-

TABLE 3

Common and unique multiple reaction monitoring transition ions generated by EETs

The bold and underlined numbers denote unique transition ions, whereas the regular numbers denote common transition ions.

5,6-EET	8,9-EET	11,12-EET	14,15-EET
191	151	167	**175**
	155	179	**219**
	167	**208**	257
	179	257	275
	183	275	301
	251	301	
	257		
	275		
	301		

dialdehyde (Fig. 6). Third, antioxidant treatment did not show an appreciable effect of viability rescue to light stress. Our results seem in contrast to a previous report showing that malondialdehyde is increased in 661W cells under exposure to visible light (66). In that report, the status of cellular reactive oxygen species is unknown, making it difficult for parallel comparison with our study. A likely discrepancy may be related to the reactive nature of the preadded synthetic chromophore, 9-*cis*-retinal, used in our study. 9-*cis*-Retinal increased the basal malondialdehyde level in dark control cells and may have introduced confounding effects that alter the oxidative status of cells.

Molecular modeling illustrates the binding of sulfaphenazole at the active site of human CYP2C9 enzyme (64), suggesting a mechanism-based inhibition. This allowed the proposal of our initial hypothesis that the CYP2C metabolic pathway would generate metabolites that induce noxious cellular responses. Human CYP2C9 and CYP2C8 as well as the respective homologous mouse CYP2C55 and CYP2C29 are able to metabolize AA and other *n*-6 polyunsaturated fatty acids into epoxy- and hydroxyeicosanoids as lipid mediators with different regioselective and enantioselective compositions (67–69). This biochemical evidence collectively suggests that sulfaphenazole may inhibit CYP2C-generated eicosanoid metabolites of AA. Alternatively, enzymatic shutdown of a CYP2C isozyme(s) by sulfaphenazole may induce a metabolic shift of AA into other oxidative metabolites. For example, inhibition of CYP2C9-generated epoxyeicosanoids by sulfaphenazole can stimulate the production of prostanoids by cyclooxygenase 2 (70). Using LC/MS, we conducted quantitative analysis of AA and investigated the effect of sulfaphenazole on production of regioisomeric EETs in 661W cells under light exposure. Light significantly increased the release of AA from membrane phospholipids (Fig. 8). To our knowledge, this is the first experimental evidence showing that photoreceptors specifically release AA under light stress. It is generally believed that most biological effects dictated by AA are attributable to its metabolites rather than the unesterified free molecule (71). This sets up the logistics for our following experiments to quantitatively measure EETs. At the functional level, this experimental effort stems from the findings that CYP2C-generated EETs can modulate the activity of cation channels (72, 73). As light triggered excessive calcium influx in 661W cells (Fig. 7), we investigated the possible association of this phenotype with production of EETs. Unfortunately, we were not able to reliably detect any one of the four *cis*-regioisomers of EETs. With the expression of CYP2C proteins (Fig. 3), this negative finding seems counterintuitive. However, the multiplicity of biochemical processing and metabolism of EETs may limit the detection sensitivity. Newly synthesized EETs can be incorporated back into membrane phospholipids through the CoA-dependent process, bind to intracellular fatty acid-binding proteins, and undergo degradation into dihydroxyeicosatrienoic acids by the soluble epoxide hydrolases, chain elongation, or β-oxidation (74), all of which may negatively affect the quantitative analysis. Nonetheless, we identified two metabolites of AA with the same molecular mass as EETs that were markedly increased both in the conditioned medium and in 661W cells under light exposure (Table 2 and Fig. 8, *D–F*). Administration of sulfaphenazole further stimulated the production of the two metabolites, suggesting a metabolic shift of AA under inhibition of the CYP2C pathway. The chemical identity of the two non-EET metabolites and their source of origin and bioactivity in cell death and survival remain to be determined. 15- and 11-hydroxyeicosatetraenoic acids generated by the lipoxygenase pathway are the plausible metabolites because they have the same molecular mass as EETs and can create certain identical transition ions under multiple reaction monitoring (75). The function of hydroxyeicosatetraenoic acids can be tissue- or cell type-specific. 15-Hydroxyeicosatetraenoic acid has been shown to demonstrate anti-inflammatory and antiapoptotic properties (76, 77).

Previous studies have shown that in addition to metabolize *n*-6 polyunsaturated fatty acids human CYP2C isozymes can also metabolize *n*-3 docosahexaenoic acid (DHA) and eicosapentaenoic acid that preferentially generate 17,18-epoxyeicosatetraenoic acid and 19,20-epoxydocosapentaenoic acid, respectively (78, 79). The biological role of these metabolites in tissues/cells and whether they synergize or antagonize the bioactive metabolites of *n*-6 fatty acids remain unclear. Photoreceptor phospholipid membranes contain a large amount of DHA in the esterified form as docosahexaenoyl- or DHA-elongated fatty acyl chains (80). The cellular pool of unesterified (free) DHA in 661W cells under light exposure is unknown. Similar to increased release of free AA under light exposure, it is of interest to know whether there is a concurrent increase of cellular free DHA and whether inhibition of the CYP2C-DHA pathway by sulfaphenazole would alter the epoxy metabolites of DHA. Previous studies have shown that oxidation enzyme-generated docosatrienes and 17*S* series resolvins from DHA are capable to reduce leukocyte infiltration and production of inflammatory cytokines (81). In the eye, neuroprotectin D1 (10,17*S*-docosatriene), a 15-lipoxygenase-1-mediated metabolite of DHA, acts as a potent cytoprotective mediator that prevents oxidative stress-induced apoptosis in retinal pigment epithelial cells (82). Currently, very little is known about self-generated, fatty acid-derived lipid mediators from either the enzyme-driven or non-enzyme-driven oxidations in photoreceptors under retinal oxidative stress. The diffusible nature of lipid mediators and the intimate functional relationships between photoreceptors and retinal pigment epithelial cells may also allow non-self-generated lipid mediators from retinal pigment epithelial cells to execute biological actions as auta-

coids on photoreceptors through modulation of receptors and/or ion channels.

A non-exclusive mechanism may co-exist to explain the cytoprotection of sulfaphenazole. Previous studies have shown that CYP2C isozymes participate in catabolic degradation of retinoic acid (RA) (83, 84). In our study, we preadded the synthetic chromophore 9-*cis*-retinal into 661W cells to increase light sensitivity. 9-*cis*-Retinal is isomerized into all-*trans*-retinal upon light exposure. Oxidation of all-*trans*-retinal by retinaldehyde dehydrogenase generates all-*trans*-RA, which can be catabolized by CYP2C isozymes into polar metabolites. All-*trans*-RA is an agonistic ligand for retinoic acid receptors and orphan nuclear receptors, which function as transcription factors that play critical roles in regulation of cell survival and growth (85, 86). In our model, administration of sulfaphenazole might slow down the catabolic rate of all-*trans*-RA, which in turn stimulates cognate nuclear receptor-mediated expression of prosurvival genes. This consideration applies to the *in vivo* role of RA-nuclear receptor signaling in maintaining homeostasis of the retina under light exposure. RA is a by-product of the visual retinoid cycle, and its level is increased in the retina upon light exposure (87). Stimulation of retinoic acid receptor activity by RA may prevent the visually toxic effect of all-*trans*-retinal (88). Thus, it is plausible that the CYP2C genes may exert regulatory control of the bioavailability of all-*trans*-RA in the retina.

In summary, we identified sulfaphenazole as a novel cytoprotective drug against toxic light-induced death of mouse-derived photoreceptors. The endogenous CYP2C55 gene and the homologous human CYP2C9 gene play a direct causative role in cell death. Our study implies that the CYP monooxygenase system needs further attention as it is a potential risk factor for retinal photodamage, especially for individuals with inherited retinal dystrophy caused by the *ABCA4* gene mutations or AMD that deposits condensation products of retinoids (89, 51). Our study lays out the foundation for *in vivo* neuroprotective evaluation of sulfaphenazole in analogous retinal disease models in animals.

Acknowledgments—We appreciate Drs. David Pepperberg and Beatrice Yue for reading the manuscript and helpful suggestions. We are also grateful to the staff of the University of Chicago Research Resource Center for assistance with flow cytometry.

REFERENCES

1. Buch, H., Vinding, T., La Cour, M., Appleyard, M., Jensen, G. B., and Nielsen, N. V. (2004) Prevalence and causes of visual impairment and blindness among 9980 Scandinavian adults: the Copenhagen City Eye Study. *Ophthalmology* **111,** 53–61
2. Al-Merjan, J. I., Pandova, M. G., Al-Ghanim M, Al-Wayel, A., and Al-Mutairi S (2005) Registered blindness and low vision in Kuwait. *Ophthalmic Epidemiol.* **12,** 251–257
3. Hata, H., Yonezawa, M., Nakanishi, T., Ri, T., and Yanashima, K. (2003) Causes of entering institutions for visually handicapped persons during the past fifteen years. *Jpn. J. Ophthalmol.* **57,** 259–262
4. Frick, K. D., Roebuck, M. C., Feldstein, J. I., McCarty, C. A., and Grover, L. L. (2012) Health services utilization and cost of retinitis pigmentosa. *Arch. Ophthalmol.* **130,** 629–634
5. Friedman, D. S., O'Colmain, B. J., Muñoz, B., Tomany, S. C., McCarty, C., de Jong, P. T., Nemesure, B., Mitchell, P., Kempen, J., and Eye Diseases Prevalence Research Group (2004) Prevalence of age-related macular degeneration in the United States. *Arch. Ophthalmol.* **122,** 564–572
6. Congdon, N., O'Colmain, B., Klaver, C. C., Klein, R., Muñoz, B., Friedman, D. S., Kempen, J., Taylor, H. R., Mitchell, P., and Eye Diseases Prevalence Research Group (2004) Causes and prevalence of visual impairment among adults in the United States. *Arch Ophthalmol.* **122,** 477–485
7. Bressler, S. B., Muñoz, B., Solomon, S. D., West, S. K., and Salisbury Eye Evaluation (SEE) Study Team (2008) Racial differences in the prevalence of age-related macular degeneration: the Salisbury Eye Evaluation (SEE) Project. *Arch. Ophthalmol.* **126,** 241–245
8. Faktorovich, E. G., Steinberg, R. H., Yasumura, D., Matthes, M. T., and LaVail, M. M. (1990) Photoreceptor degeneration in inherited retinal dystrophy delayed by basic fibroblast growth factor. *Nature* **347,** 83–86
9. Frasson, M., Picaud, S., Léveillard, T., Simonutti, M., Mohand-Said, S., Dreyfus, H., Hicks, D., and Sabel, J. (1999) Glial cell line-derived neurotrophic factor induces histologic and functional protection of rod photoreceptors in the rd/rd mouse. *Invest. Ophthalmol. Vis. Sci.* **40,** 2724–2734
10. Cayouette, M., Behn, D., Sendtner, M., Lachapelle, P., and Gravel, C. (1998) Intraocular gene transfer of ciliary neurotrophic factor prevents death and increases responsiveness of rod photoreceptors in the retinal degeneration slow mouse. *J. Neurosci.* **18,** 9282–9293
11. Koch, S., Sothilingam, V., Garcia Garrido, M., Tanimoto, N., Becirovic, E., Koch, F., Seide, C., Beck, S. C., Seeliger, M. W., Biel, M., Mühlfriedel, R., and Michalakis, S. (2012) Gene therapy restores vision and delays degeneration in the CNGB1−/− mouse model of retinitis pigmentosa. *Hum. Mol. Genet.* **21,** 4486–4496
12. Pang, J. J., Boye, S. L., Kumar, A., Dinculescu, A., Deng, W., Li, J., Li, Q., Rani, A., Foster, T. C., Chang, B., Hawes, N. L., Boatright, J. H., and Hauswirth, W. W. (2008) AAV-mediated gene therapy for retinal degeneration in the rd10 mouse containing a recessive PDEβ mutation. *Invest. Ophthalmol. Vis. Sci.* **49,** 4278–4283
13. Komeima, K., Rogers, B. S., Lu, L., and Campochiaro, P. A. (2006) Antioxidants reduce cone cell death in a model of retinitis pigmentosa. *Proc. Natl. Acad. Sci. U.S.A.* **103,** 11300–11305
14. Otani, A., Dorrell, M. I., Kinder, K., Moreno, S. K., Nusinowitz, S., Banin, E., Heckenlively, J., and Friedlander, M. (2004) Rescue of retinal degeneration by intravitreally injected adult bone marrow-derived lineage-negative hematopoietic stem cells. *J. Clin. Investig.* **114,** 765–774
15. Berson, E. L., Rosner, B., Sandberg, M. A., Hayes, K. C., Nicholson, B. W., Weigel-DiFranco, C., and Willett, W. (1993) A randomized trial of vitamin A and vitamin E supplementation for retinitis pigmentosa. *Arch. Ophthalmol.* **111,** 761–772
16. Radu, R. A., Yuan, Q., Hu, J., Peng, J. H., Lloyd M, Nusinowitz, S., Bok, D., and Travis, G. H. (2008) Accelerated accumulation of lipofuscin pigments in the RPE of a mouse model for ABCA4-mediated retinal dystrophies following vitamin A supplementation. *Invest. Ophthalmol. Vis. Sci.* **49,** 3821–3829
17. Rosenfeld, P. J., Brown, D. M., Heier, J. S., Boyer, D. S., Kaiser, P. K., Chung, C. Y., Kim, R. Y., and MARINA Study Group. (2006) Ranibizumab for neovascular age-related macular degeneration. *N. Engl. J. Med.* **355,** 1419–1431
18. Hollyfield, J. G., Bonilha, V. L., Rayborn, M. E., Yang, X., Shadrach, K. G., Lu, L., Ufret, R. L., Salomon, R. G., and Perez, V. L. (2008) Oxidative damage-induced inflammation initiates age-related macular degeneration. *Nat. Med.* **14,** 194–198
19. Ding, X., Patel, M., and Chan, C. C. (2009) Molecular pathology of age-related macular degeneration. *Prog. Retin. Eye Res.* **28,** 1–18
20. Chew, E. Y., Clemons, T. E., Agrón, E., Sperduto, R. D., Sangiovanni, J. P., Kurinij, N., Davis, M. D., and Age-Related Eye Disease Study Research Group. (2013) Long-term effects of vitamins C and E, β-carotene, and zinc on age-related macular degeneration: AREDS Report No. 35. *Ophthalmology* **120,** 1604–11.e4
21. Pollitt, S. K., Pallos, J., Shao, J., Desai, U. A., Ma, A. A., Thompson, L. M., Marsh, J. L., and Diamond, M. I. (2003) A rapid cellular FRET assay of polyglutamine aggregation identifies a novel inhibitor. *Neuron* **40,** 685–694

22. Bush, E., Fielitz, J., Melvin, L., Martinez-Arnold, M., McKinsey, T. A., Plichta, R., and Olson, E. N. (2004) A small molecular activator of cardiac hypertrophy uncovered in a chemical screen for modifiers of the calcineurin signaling pathway. *Proc. Natl. Acad. Sci. U.S.A.* **101,** 2870–2875
23. Gupta, P. B., Onder, T. T., Jiang, G., Tao, K., Kuperwasser, C., Weinberg, R. A., and Lander, E. S. (2009) Identification of selective inhibitors of cancer stem cells by high-throughput screening. *Cell* **138,** 645–659
24. Somwar, R., Shum, D., Djaballah, H., and Varmus, H. (2009) Identification and preliminary characterization of novel small molecules that inhibit growth of human lung adenocarcinoma cells. *J. Biomol. Screen* **14,** 1176–1184
25. Degterev, A., Huang, Z., Boyce, M., Li, Y., Jagtap, P., Mizushima, N., Cuny, G. D., Mitchison, T. J., Moskowitz, M. A., and Yuan, J. (2005) Chemical inhibitor of nonapoptotic cell death with therapeutic potential for ischemic brain injury. *Nat. Chem. Biol.* **1,** 112–119
26. Kepp, O., Galluzzi, L., Lipinski, M., Yuan, J., and Kroemer, G. (2011) Cell death assays for drug discovery. *Nat. Rev. Drug Discov.* **10,** 221–237
27. Paskowitz, D. M., LaVail, M. M., and Duncan, J. L. (2006) Light and inherited retinal degeneration. *Br. J. Ophthalmol.* **90,** 1060–1066
28. Kijas, J. W., Cideciyan, A. V., Aleman, T. S., Pianta M. J., Pearce-Kelling, S. E., Miller, B. J., Jacobson, S. G., Aguirre, G. D., and Acland, G. M. (2002) Naturally occurring rhodopsin mutation in the dog causes retinal dysfunction and degeneration mimicking human dominant retinitis pigmentosa. *Proc. Natl. Acad. Sci. U.S.A.* **99,** 6328–6333
29. Naash, M. L., Peachey, N. S., Li, Z. Y., Gryczan, C. C., Goto, Y., Blanks, J., Milam, A. H., and Ripps, H. (1996) Light induced acceleration of photoreceptor degeneration in transgenic mice expressing mutant rhodopsin. *Invest. Ophthalmol. Vis. Sci.* **37,** 775–782
30. Wenzel, A., Grimm, C., Samardzija, M., and Remé, C. E. (2005) Molecular mechanisms of light-induced photoreceptor apoptosis and neuroprotection for retinal degeneration. *Prog. Retin. Eye Res.* **24,** 275–306
31. Marc, R. E., Jones, B. W., Watt, C. B., Vazquez-Chona, F., Vaughan, D. K., and Organisciak, D. T. (2008) Extreme retinal remodeling triggered by light damage: implications for age related macular degeneration. *Mol. Vis.* **14,** 782–806
32. Rutar, M., Provis, J. M., and Valter, K. (2010) Brief exposure to damaging light causes focal recruitment of macrophages, and long-term destabilization of photoreceptors in the albino rat retina. *Curr. Eye Res.* **35,** 631–643
33. Rutar, M., Natoli, R., Kozulin, P., Valter, K., Gatenby, P., and Provis, J. M. (2011) Analysis of complement expression in light-induced retinal degeneration: synthesis and deposition of C3 by microglia/macrophages is associated with focal photoreceptor degeneration. *Invest. Ophthalmol. Vis. Sci.* **52,** 5347–5358
34. Chang, Q., Peter, M. E., and Grassi, M. A. (2012) Fas ligand-Fas signaling participates in light-induced apoptotic death in photoreceptor cells. *Invest. Ophthalmol. Vis. Sci.* **53,** 3703–3716
35. Zhang, J. H., Chung, T. D., and Oldenburg, K. R. (1999) A simple statistical parameter for use in evaluation and validation of high throughput screening assays. *J. Biomol. Screen.* **4,** 67–73
36. Bligh, E. G., and Dyer, W. J. (1959) A rapid method of total lipid extraction and purification. *Can. J. Biochem. Physiol.* **37,** 911–917
37. Farber, D. B. (1995) From mice to men: the cyclic GMP phosphodiesterase gene in vision and disease. *Invest. Ophthalmol. Vis. Sci.* **36,** 263–275
38. Barabas, P., Cutler Peck, C., and Krizaj, D. (2010) Do calcium channel blockers rescue dying photoreceptors in the Pde6b (rd1) mouse? *Adv. Exp. Med. Biol.* **664,** 491–499
39. Wu, H., Cowing, J. A., Michaelides, M., Wilkie, S. E., Jeffery, G., Jenkins, S. A., Mester, V., Bird, A. C., Robson, A. G., Holder, G. E., Moore, A. T., Hunt, D. M., and Webster, A. R. (2006) Mutations in the gene KCNV2 encoding a voltage-gated potassium channel subunit cause "cone dystrophy with supernormal rod electroretinogram" in humans. *Am. J. Hum. Genet.* **79,** 574–579
40. Babai, N., and Thoreson, W. B. (2009) Horizontal cell feedback regulates calcium currents and intracellular calcium levels in rod photoreceptors of salamander and mouse retina. *J. Physiol.* **587,** 2353–2364
41. Ogilvie, J. M., and Speck, J. D. (2002) Dopamine has a critical role in photoreceptor degeneration in the rd mouse. *Neurobiol. Dis.* **10,** 33–40
42. Bubenik, G. A., and Purtill, R. A. (1980) The role of melatonin and dopamine in retinal physiology. *Can. J. Physiol. Pharmacol.* **58,** 1457–1462
43. Wiechmann, A. F., and O'Steen, W. K. (1992) Melatonin increases photoreceptor susceptibility to light-induced damage. *Invest. Ophthalmol. Vis. Sci.* **33,** 1894–1902
44. Sugawara, T., Sieving, P. A., Iuvone, P. M., and Bush, R. A. (1998) The melatonin antagonist luzindole protects retinal photoreceptors from light damage in the rat. *Invest. Ophthalmol. Vis. Sci.* **39,** 2458–2465
45. Nguyen-Legros, J., Chanut, E., Versaux-Botteri, C., Simon, A., and Trouvin, J. H. (1996) Dopamine inhibits melatonin synthesis in photoreceptor cells through a D2-like receptor subtype in the rat retina: biochemical and histochemical evidence. *J. Neurochem.* **67,** 2514–2520
46. Cohen, A. I., Todd, R. D., Harmon, S., and O'Malley, K. L. (1992) Photoreceptors of mouse retinas possess D4 receptors coupled to adenylate cyclase. *Proc. Natl. Acad. Sci. U.S.A.* **89,** 12093–12097
47. Wenzel, A., Grimm, C., Seeliger, M. W., Jaissle, G., Hafezi, F., Kretschmer, R., Zrenner, E., and Remé, C. E. (2001) Prevention of photoreceptor apoptosis by activation of the glucocorticoid receptor. *Invest. Ophthalmol. Vis. Sci.* **42,** 1653–1659
48. Zhang, C., Lei, B., Lam, T. T., Yang, F., Sinha, D., and Tso, M. O. (2004) Neuroprotection of photoreceptors by minocycline in light-induced retinal degeneration. *Invest. Ophthalmol. Vis. Sci.* **45,** 2753–2759
49. Yang, L. P., Zhu, X. A., and Tso, M. O. (2007) A possible mechanism of microglia-photoreceptor crosstalk. *Mol. Vis.* **13,** 2048–2057
50. Biber, K., Neumann, H., Inoue, K., and Boddeke, H. W. (2007) Neuronal 'on' and 'off' signals control microglia. *Trends Neurosci.* **30,** 596–602
51. Chen, Y., Okano, K., Maeda, T., Chauhan, V., Golczak, M., Maeda, A., and Palczewski, K. (2012) Mechanism of all-*trans*-retinal toxicity with implications for Stargardt disease and age-related macular degeneration. *J. Biol. Chem.* **287,** 5059–5069
52. Bursch, W., Hochegger, K., Torok, L., Marian, B., Ellinger, A., and Hermann, R. S. (2000) Autophagic and apoptotic types of programmed cell death exhibit different fates of cytoskeletal filaments. *J. Cell Sci.* **113,** 1189–1198
53. Hall, A. (1998) Rho GTPases and the actin cytoskeleton. *Science* **279,** 509–514
54. Tanito, M., Masutani, H., Kim, Y. C., Nishikawa, M., Ohira, A., and Yodoi, J. (2005) Sulforaphane induces thioredoxin through the antioxidant-responsive element and attenuates retinal light damage in mice. *Invest. Ophthalmol. Vis. Sci.* **46,** 979–987
55. Neve, E. P., and Ingelman-Sundberg, M. (2008) Intracellular transport and localization of microsomal cytochrome P450. *Anal. Bioanal. Chem.* **392,** 1075–1084
56. Gonzalez, F. J. (2005) Role of cytochromes P450 in chemical toxicity and oxidative stress: studies with CYP2E1. *Mutat. Res.* **569,** 101–110
57. Zangar, R. C., Davydov, D. R., and Verma, S. (2004) Mechanisms that regulate production of reactive oxygen species by cytochrome P450. *Toxicol. Appl. Pharmacol.* **199,** 316–331
58. Penn, J. S., Naash, M. I., and Anderson, R. E. (1987) Effect of light history on retinal antioxidants and light damage susceptibility in the rat. *Exp. Eye Res.* **44,** 779–788
59. Tanito, M., Nishiyama, A., Tanaka, T., Masutani, H., Nakamura, H., Yodoi, J., and Ohira, A. (2002) Change of redox status and modulation by thiol replenishment in retinal photooxidative damage. *Invest. Ophthalmol. Vis. Sci.* **43,** 2392–2400
60. Jung, H., and Remé, C. (1994) Light-evoked arachidonic acid release in the retina: illuminance/duration dependence and the effects of quinacrine, mellitin and lithium. Light-evoked arachidonic acid release. *Graefes Arch. Clin. Exp. Ophthalmol.* **232,** 167–175
61. Kolko, M., Christoffersen, N. R., Barreiro, S. G., and Bazan, N. G. (2004) Expression and location of mRNAs encoding multiple forms of secretory phospholipase A2 in the rat retina. *J. Neurosci. Res.* **77,** 517–524
62. Rzigalinski, B. A., Willoughby, K. A., Hoffman, S. W., Falck, J. R., and Ellis, E. F. (1999) Calcium influx factor, further evidence it is 5,6-epoxyeicosatrienoic acid. *J. Biol. Chem.* **274,** 175–182
63. Berridge, M. J., Lipp, P., and Bootman, M. D. (2000) The versatility and universality of calcium signalling. *Nat. Rev. Mol. Cell Biol.* **1,** 11–21
64. Trump, B. F., and Berezesky, I. K. (1996) The role of altered $[Ca^{2+}]_i$ regulation in apoptosis, oncosis, and necrosis. *Biochim. Biophys. Acta* **1313,**

173–178
65. Mancy, A., Dijols, S., Poli, S., Guengerich, P., and Mansuy, D. (1996) Interaction of sulfaphenazole derivatives with human liver cytochromes P450 2C: molecular origin of the specific inhibitory effects of sulfaphenazole on CYP 2C9 and consequences for the substrate binding site topology of CYP 2C9. *Biochemistry* **35,** 16205–16212
66. Krishnamoorthy, R. R., Crawford, M. J., Chaturvedi, M. M., Jain, S. K., Aggarwal, B. B., Al-Ubaidi, M. R., and Agarwal, N. (1999) Photo-oxidative stress down-modulates the activity of nuclear factor-κB via involvement of caspase-1, leading to apoptosis of photoreceptor cells. *J. Biol. Chem.* **274,** 3734–3743
67. Daikh, B. E., Lasker, J. M., Raucy, J. L., and Koop, D. R. (1994) Regio- and stereoselective epoxidation of arachidonic acid by human cytochromes P450 2C8 and 2C9. *J. Pharmacol. Exp. Ther.* **271,** 1427–1433
68. Wang, H., Zhao, Y., Bradbury, J. A., Graves, J. P., Foley, J., Blaisdell, J. A., Goldstein, J. A., and Zeldin, D. C. (2004) Cloning, expression, and characterization of three new mouse cytochrome P450 enzymes and partial characterization of their fatty acid oxidation activities. *Mol. Pharmacol.* **65,** 1148–1158
69. Luo, G., Zeldin, D. C., Blaisdell, J. A., Hodgson, E., and Goldstein, J. A. (1998) Cloning and expression of murine CYP2Cs and their ability to metabolize arachidonic acid. *Arch. Biochem. Biophys.* **357,** 45–57
70. Michaelis, U. R., Falck, J. R., Schmidt, R., Busse, R., and Fleming, I. (2005) Cytochrome P4502C9-derived epoxyeicosatrienoic acids induce the expression of cyclooxygenase-2 in endothelial cells. *Arterioscler. Thromb. Vasc. Biol.* **25,** 321–326
71. Caro, A. A., and Cederbaum, A. I. (2006) Role of cytochrome P450 in phospholipase A2- and arachidonic acid-mediated cytotoxicity. *Free Radic. Biol. Med.* **40,** 364–375
72. Vriens, J., Owsianik, G., Fisslthaler, B., Suzuki, M., Janssens, A., Voets, T., Morisseau, C., Hammock, B. D., Fleming, I., Busse, R., and Nilius, B. (2005) Modulation of the Ca^2 permeable cation channel TRPV4 by cytochrome P450 epoxygenases in vascular endothelium. *Circ. Res.* **97,** 908–915
73. Fleming, I., Rueben, A., Popp, R., Fisslthaler, B., Schrodt, S., Sander, A., Haendeler, J., Falck, J. R., Morisseau, C., Hammock, B. D., and Busse, R. (2007) Epoxyeicosatrienoic acids regulate Trp channel dependent Ca^{2+} signaling and hyperpolarization in endothelial cells. *Arterioscler. Thromb. Vasc. Biol.* **27,** 2612–2618
74. Spector, A. A., Fang, X., Snyder, G. D., and Weintraub, N. L. (2004) Epoxyeicosatrienoic acids (EETs): metabolism and biochemical function. *Prog. Lipid Res.* **43,** 55–90
75. Dumlao, D. S., Buczynski, M. W., Norris, P. C., Harkewicz, R., and Dennis, E. A. (2011) High-throughput lipidomic analysis of fatty acid derived eicosanoids and N-acylethanolamines. *Biochim. Biophys. Acta* **1811,** 724–736
76. Krönke, G., Katzenbeisser, J., Uderhardt, S., Zaiss, M. M., Scholtysek, C., Schabbauer, G., Zarbock, A., Koenders, M. I., Axmann, R., Zwerina, J., Baenckler, H. W., van den Berg, W., Voll, R. E., Kühn, H., Joosten, L. A., and Schett, G. (2009) 12/15-Lipoxygenase counteracts inflammation and tissue damage in arthritis. *J. Immunol.* **183,** 3383–3389
77. Tang, D. G., Chen, Y. Q., Honn, K. V. (1996) Arachidonate lipoxygenases as essential regulators of cell survival and apoptosis. *Proc. Natl. Acad. Sci. U.S.A.* **93,** 5241–5246
78. Arnold, C., Markovic, M., Blossey, K., Wallukat, G., Fischer, R., Dechend, R., Konkel, A., von Schacky, C., Luft, F. C., Muller, D. N., Rothe, M., and Schunck, W. H. (2010) Arachidonic acid-metabolizing cytochrome P450 enzymes are targets of ω-3 fatty acids. *J. Biol. Chem.* **285,** 32720–32733
79. Fer, M., Dréano, Y., Lucas, D., Corcos, L., Salaün J. P., Berthou, F., and Amet, Y. (2008) Metabolism of eicosapentaenoic and docosahexaenoic acids by recombinant human cytochromes P450. *Arch. Biochem. Biophys.* **471,** 116–125
80. Bazan, N. G., Calandria, J. M., and Serhan, C. N. (2010) Rescue and repair during photoreceptor cell renewal mediated by docosahexaenoic acid-derived neuroprotectin D1. *J. Lipid Res.* **51,** 2018–2031
81. Hong, S., Gronert, K., Devchand, P.R., Moussignac, R. L., and Serhan, C. N. (2003) Novel docosatrienes and 17*S*-resolvins generated from docosahexaenoic acid in murine brain, human blood, and glial cells. Autacoids in anti-inflammation. *J. Biol. Chem.* **278,** 14677–14687
82. Mukherjee, P. K., Marcheselli, V. L., Serhan, C. N., and Bazan, N. G. (2004) Neuroprotectin D1: a docosahexaenoic acid-derived docosatriene protects human retinal pigment epithelial cells from oxidative stress. *Proc. Natl. Acad. Sci. U.S.A.* **101,** 8491–8496
83. Qian, L., Zolfaghari, R., and Ross, A. C. (2010) Liver-specific cytochrome P450 CYP2C22 is a direct target of retinoic acid and a retinoic acid-metabolizing enzyme in rat liver. *J. Lipid Res.* **51,** 1781–1792
84. Marill, J., Cresteil, T., Lanotte, M., and Chabot, G. G. (2000) Identification of human cytochrome P450s involved in the formation of all-*trans*-retinoic acid principal metabolites. *Mol. Pharmacol.* **58,** 1341–1348
85. de Lera, A. R., Bourguet, W., Altucci, L., and Gronemeyer, H. (2007) Design of selective nuclear receptor modulators: RAR and RXR as a case study. *Nat. Rev. Drug Discov.* **6,** 811–820
86. Schug, T. T., Berry, D. C., Shaw, N. S., Travis, S. N., and Noy, N. (2007) Opposing effects of retinoic acid on cell growth result from alternate activation of two different nuclear receptors. *Cell* **129,** 723–733
87. McCaffery, P., Mey, J., and Dräger, U. C. (1996) Light-mediated retinoic acid production. *Proc. Natl. Acad. Sci. U.S.A.* **93,** 12570–12574
88. Maeda, A., Golczak, M., Maeda, T., and Palczewski, K. (2009) Limited roles of Rdh8, Rdh12, and Abca4 in all-*trans*-retinal clearance in mouse retina. *Invest. Ophthalmol. Vis. Sci.* **50,** 5435–5443
89. Sparrow, J. R., Fishkin, N., Zhou, J., Cai, B., Jang, Y. P., Krane, S., Itagaki, Y., and Nakanishi, K. (2003) A2E, a byproduct of the visual cycle. *Vision Res.* **43,** 2983–2990
90. Williams, P. A., Cosme, J., Ward, A., Angove, H. C., Matak Vinković, D., and Jhoti, H. (2003) Crystal structure of human cytochrome P450 2C9 with bound warfarin. *Nature* **424,** 464–468